8th BRNO EFEPR SCHOOL

Piotr Pietrzyk

Jagiellonian University in Krakow, Poland

pietrzyk@chemia.uj.edu.pl

Application of EPR to materials, surfaces, and powders

CEITEC

www.eprschool.ceitec.cz

EFEPR

gallery of heterogeneous materials with reduced dimensionality

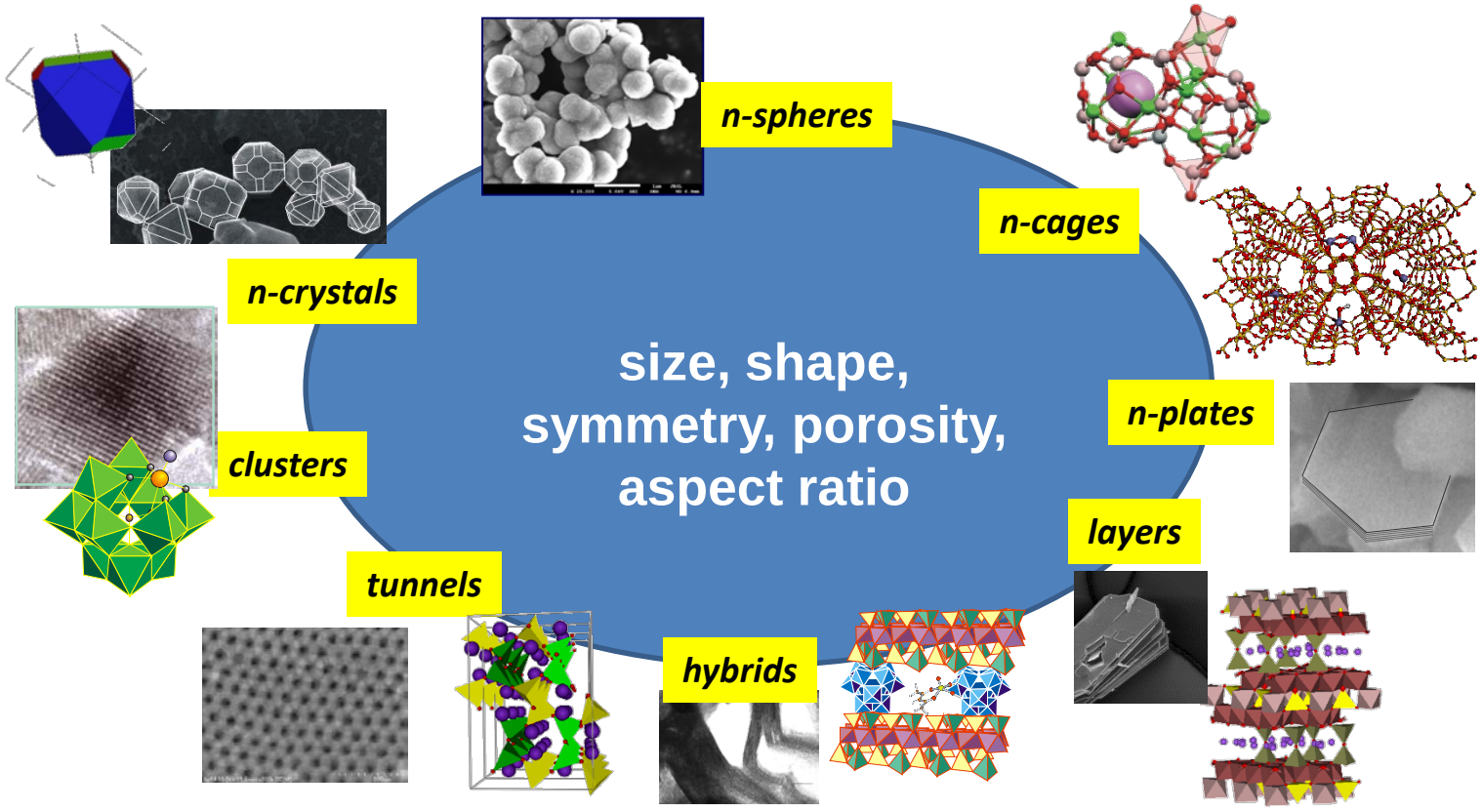

chemical and magnetic functionalization by TMI – spin phenomena at interfaces associated with reactivity

surface complexes – symmetry and speciation

crystalline
3D nanoporous
tectosilicates

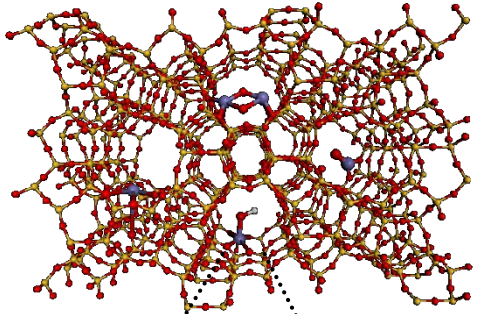

heteroleptic cage complex
(*reticular species*)

microheterogeneity
speciation

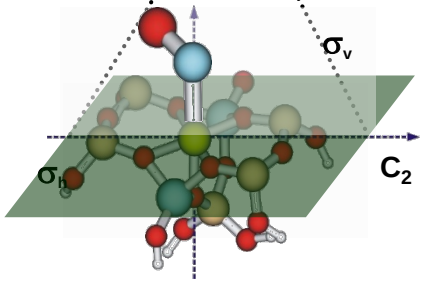

epitoms
(*cluster model*)

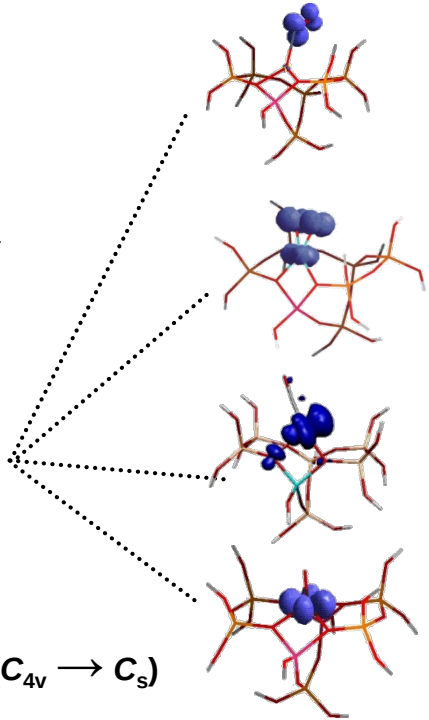

magnetophore

symmetry is often lowered upon coordination ($C_{4v} \longrightarrow C_s$)

heterogeneity of surface and the presence of heteroleptic ligands gives rise to low symmetry and pronounced speciation (distribution of EPR parameters, strain effects) resulting in complex EPR spectra

8th BRNO EFEPR SCHOOL

chemical species in disordered systems detected with EPR

paramagnets = atoms, molecules, solids containing net unpaired electrons (magnetic moments)

some simple adsorbed molecules with unpaired electrons (NO, NO_2, O_2)

transition-metal ion complexes (molecular and supported)

electronic defects in solids

electrons of conducting bands

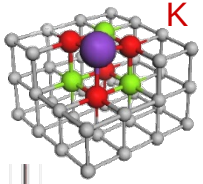

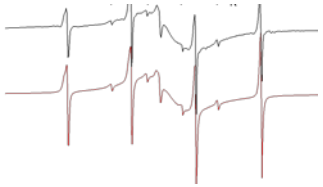

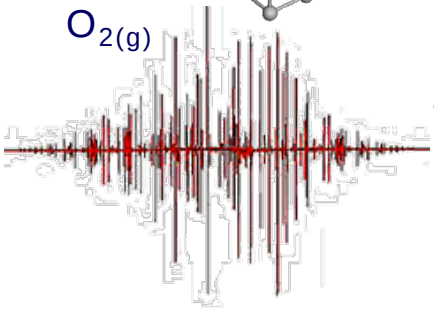

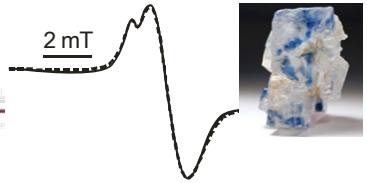

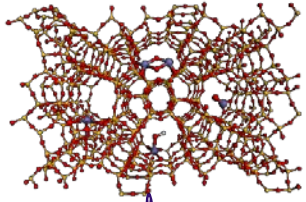

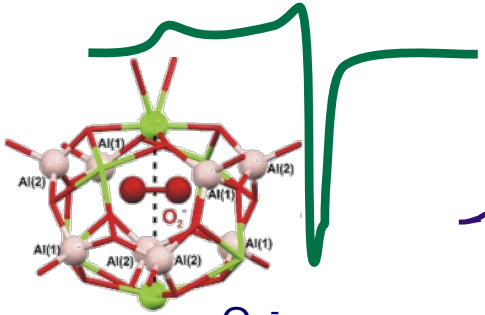

O_2^-

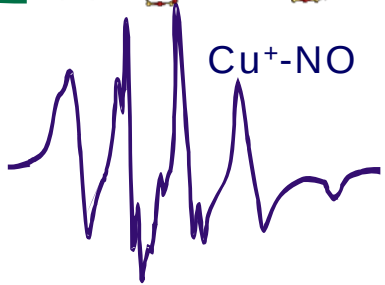

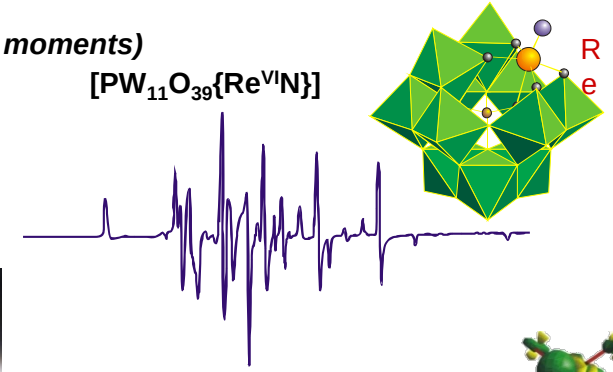

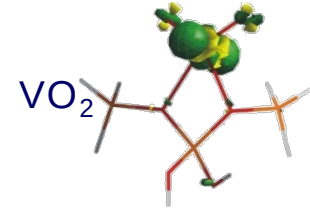

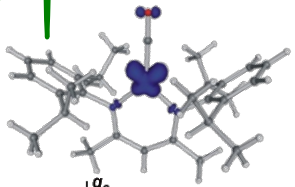

Ni+CO-diketimine

8th BRNO EFEPR SCHOOL

EPR profits

identification

$$Y(B,\nu) = C \int_{\theta}^{\pi/2} \int_{\varphi}^{2\pi} \sum_{i} P(i,\theta,\varphi,\nu)\, f(B - B_0[\nu], \sigma_B)\, \mathrm{d}\cos\theta\, \mathrm{d}\varphi$$

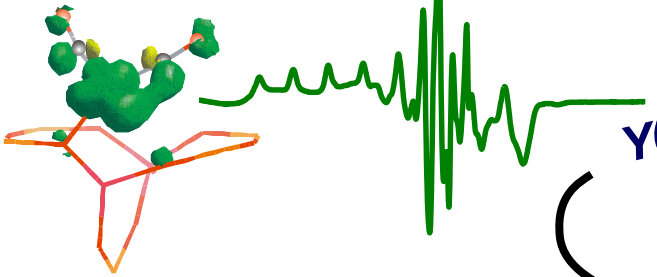

spatial distribution (imaging)

$$I(B) = \int_{-\infty}^{+\infty} (S(B - r \cdot grad_r B) \cdot P(r) \cdot C(r))\, dr$$

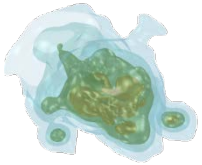

www.novilet.eu

ERI TM600 scanner

$B = B_o + r \text{ grad } B$

$Y(B)dB \rightarrow I(x,y,z)$

$I = \iint Y(B)dB \xrightarrow{B = \text{const}} I(t)$

dynamic phenomena

quantification (analytics)

$$N_x = \frac{g_w^2\,[S(S+1)]_w h_w Q_x H_m^{\,w}\, G_w P_w^{0.5}}{g_x^2\,[S(S+1)]_x h_x Q_x H_m^{\,x}\, G_x P_x^{0.5}} \left(\frac{A_x}{A_w} N_w\right)$$

rate processes (kinetics)

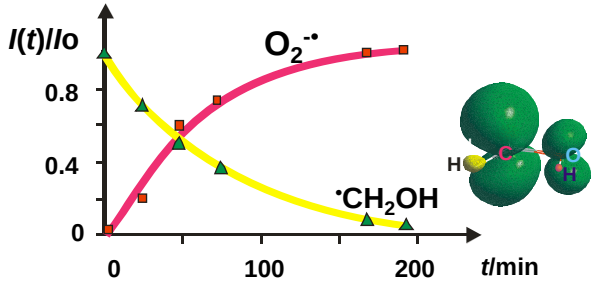

8th BRNO EFEPR SCHOOL

outline

1. EPR spectra of anisotropic systems
   - *isotropic and anisotropic spectra*
   - *powder systems*
   - *angular dependancy of g factor*
   - *symmetry of EPR spectrum*
2. Extra features of powder EPR spectra of anisotropic systems
3. Low-symmetry effects
4. Local inhomogeneity – strain effects
5. Local symmetry probes

8th BRNO EFEPR SCHOOL

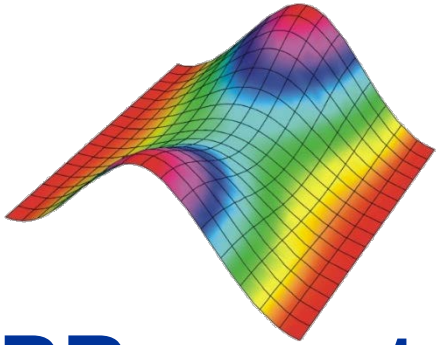

EPR spectra of anisotropic systems

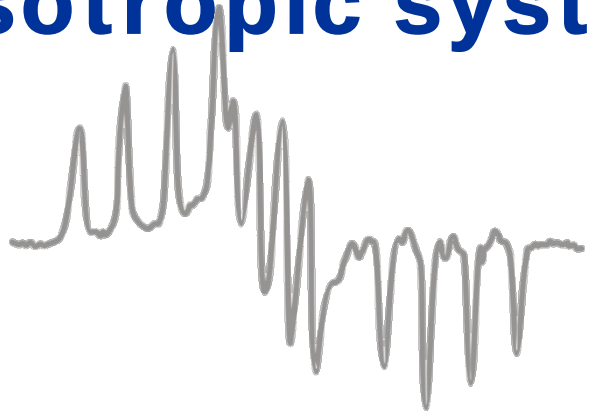

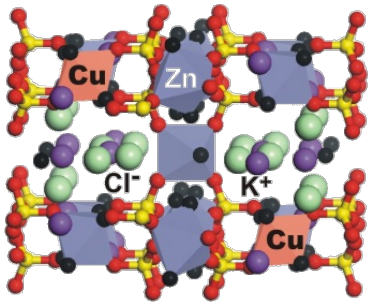

8th BRNO EFEPR SCHOOL

isotropic spectra

Isotropic = „same in all directions”

g is a scalar

$$\vec{\mu} = -g_{iso}(\mu_B/\hbar)\vec{S}$$

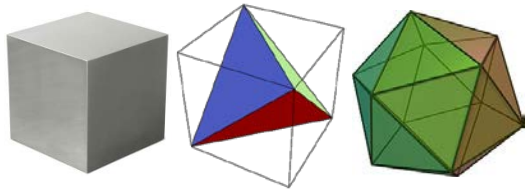

- In fluid solution a molecule can tumble rapidly, and
- presents an „average” to the external magnetic field direction.
- An „average (or isotropic) response is detected,
- provided that the tumbling is fast compared to the frequency of the experiment.

partially time-averaged spectra- asymmetric line broadening

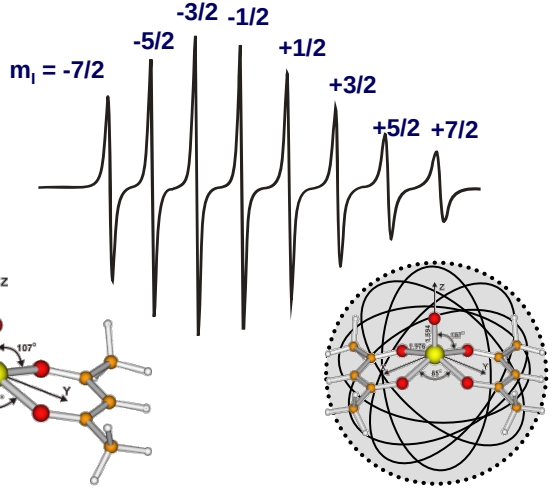

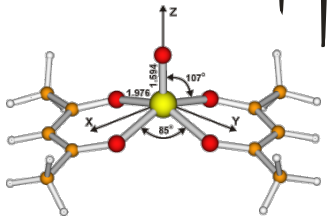

VO(acac)$_2$

$\tau_R = \eta V/kT$

high local symmetry (T, T_h, T_d, O, O_h, I_h, … R_3)

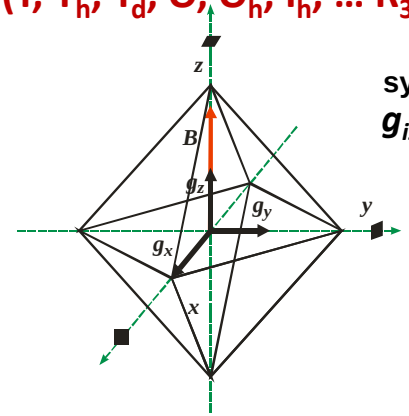

symmetry constraints

$g_{iso} = g_{xx} = g_{yy} = g_{zz}$

$$H = \hbar^{-1} g_{iso} \mu_B B^T \cdot S$$

$$H = \hbar^{-1} g \mu_B (B_x S_x + B_y S_y + B_z S_z)$$

8th BRNO EFEPR SCHOOL

$Cu(acac)_2$ solution spectrum

$Cu(acac)_2$ $(3d^9)$

^{63}Cu $I = 3/2$ $g_n = 1.484$ Ab = 69.2%

^{65}Cu $I = 3/2$ $g_n = 1.588$ Ab = 30.8%

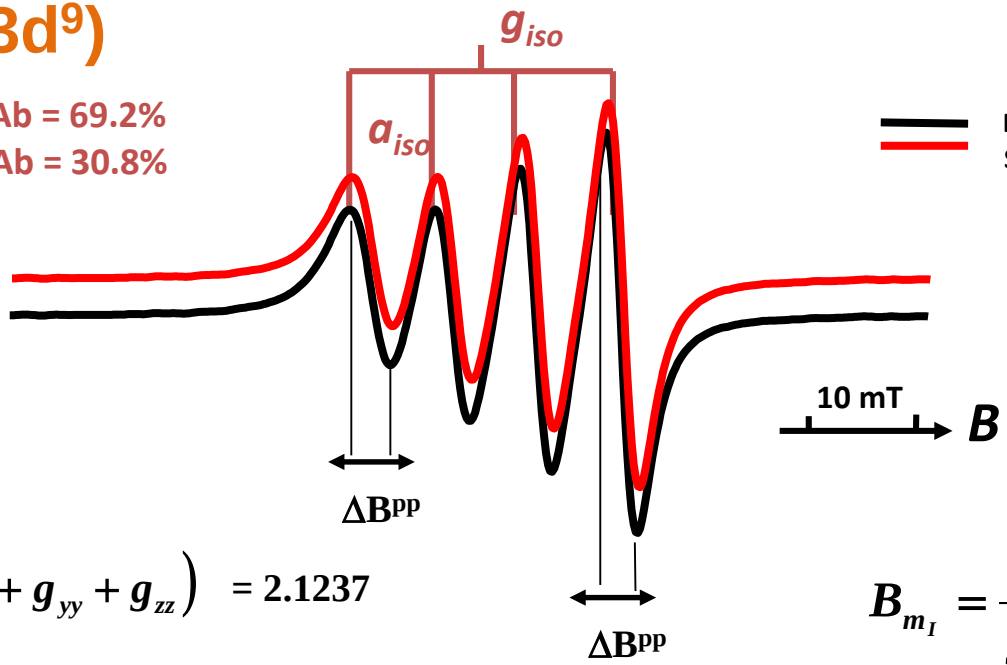

$$\langle g \rangle = \frac{1}{3}\left(g_{xx} + g_{yy} + g_{zz}\right) = 2.1237$$

$$\langle A \rangle = \frac{1}{3}\left(A_{xx} + A_{yy} + A_{zz}\right) = a_{iso} = 7.62\ \text{mT}$$

$$B_{m_I} = \frac{h\nu_0}{g\mu_B} - \frac{a_{iso} m_I}{g\mu_B}$$

note that linewidths are not constant

$Cu(acac)_2$ solution spectrum

$Cu(acac)_2$ $(3d^9)$

^{63}Cu $I = 3/2$ $g_n = 1.484$ Ab = 69.2%

^{65}Cu $I = 3/2$ $g_n = 1.588$ Ab = 69.2%

m_I-dependence of linewidths results from incomplete averaging of g and A tensor anisotropy

$$\Delta B_{pp} = \alpha + \sum_i \left(\beta_i m_i + \gamma_i m_i^2 + \ldots\right)$$

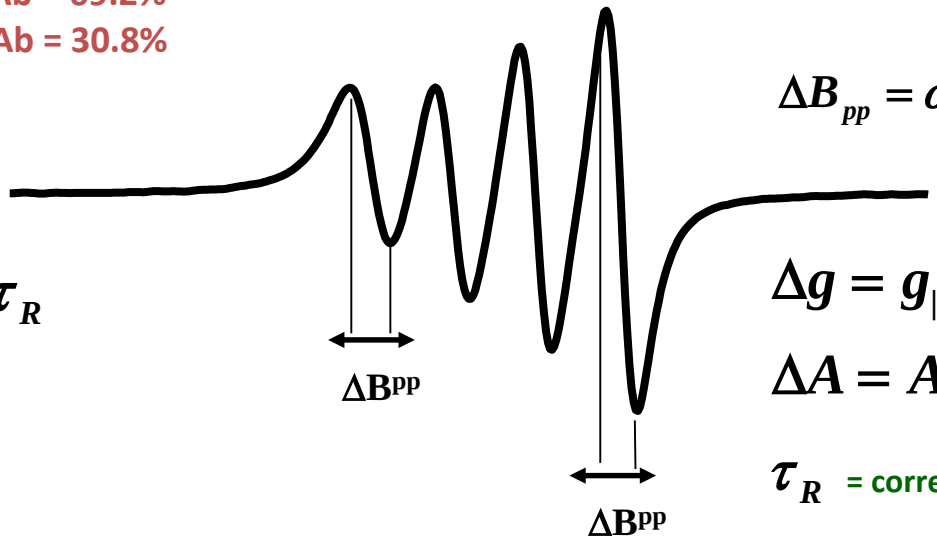

$$\alpha - \alpha_0 \propto (\Delta g)^2 \tau_R$$

$$\beta_i \propto (\Delta g \Delta A) \tau_R$$

$$\gamma_i \propto (\Delta A)^2 \tau_R$$

$$\Delta g = g_{\parallel} - g_{\perp}$$

$$\Delta A = A_{\parallel} - A_{\perp}$$

τ_R = correlation rotation time

for a spherical particle of radius r

$$\tau_R = \frac{4\pi r^3 \eta}{3kT}$$

J. Chem. Phys., 33, 1094, (1960), 44, 154, (1966); 44, 169, (1966)

frozen solution „powder” spectrum

$Cu(acac)_2$ $(3d^9)$

^{63}Cu $I = 3/2$ $g_n = 1.484$ Ab = 69.2%
^{65}Cu $I = 3/2$ $g_n = 1.588$ Ab = 30.8%

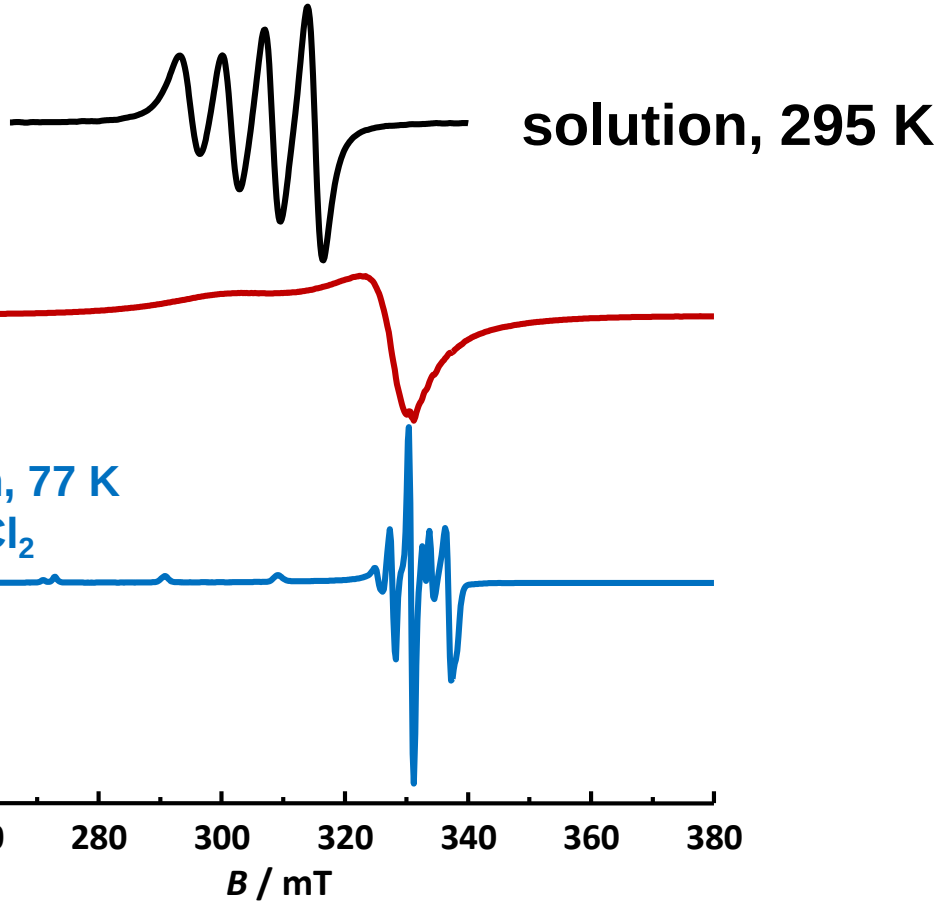

anisotropic spectra

g is a tensor

$$\vec{\mu} = -(\mu_B/\hbar)\, g\vec{S}$$

$$g = \begin{bmatrix} g_{xx} & 0 & 0 \\ 0 & g_{yy} & 0 \\ 0 & 0 & g_{zz} \end{bmatrix}$$

local symmetry lower than
(T, T_h, T_d, O, O_h, I_h, … R_3)

Anisotropic = „different in different directions"

- In a solid sample molecular motion is usually restricted,
- often only vibrational motion remains.
- EPR spectra reflect a „sum" of many molecular orientations with respect to the applied magnetic field,
- ideally stochastic distribution is expected.

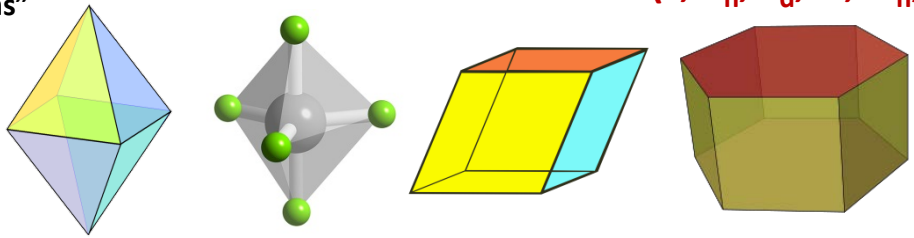

symmetry constraints

$g_{xx} = g_{yy} \neq g_{zz}$

$g_{xx} \neq g_{yy} \neq g_{zz}$

$$\boldsymbol{H} = \hbar^{-1}\, \mu_B \boldsymbol{B}^T \cdot \boldsymbol{g} \cdot \boldsymbol{S}$$

$$\boldsymbol{H} = \hbar^{-1}\, \mu_B (g_{xx} B_x S_x + g_{yy} B_y S_y + g_{zz} B_z S_z)$$

powder-like systems for EPR measurements

preparation of a sample in a „powder" form

1) **The paramagnetic must be diluted without being contaminated. Dilution must be obtained at the molecular level.**

2) **The orientation of paramagnetic particles in space must be completely stochastic. The solid phase must be obtained in a form sufficiently fine to avoid the presence of macrocrystalites. In the case of frozen solutions, these must form a glass.**

3) **The random orientation of the paramagnets must be tested by rotating the sample in EPR cavity of about 20° and repeating the measurement. If the two spectra are identical, the sample can be considered as a powder one.**

powder-like systems for EPR measurements

preparation of a sample in the form of glass „powder”

Mixtures

Components	*Ratio A:B:C...*
hydrocarbon	
3-methylpentane/isopentane	1:1
isopentane/methylcyclohexane	1:6
methylcyclopentane/methylcyclohexane	1:1
3-methylpentane/isopentane	1:2
alcohol	
ethanol/methanol	4:1, 5:2, 1:9
isopropanol/isopentane	3:7
ethanol/ispopentane/diethyl ether	2:5:5
isopentane/n-butanol	7:3
isopentane/isopropanol	8:2
diethyl ether/isooctane/isopropanol (or ethanol)	3:3:1
diethyl ether/isopropanol (or ethanol)	3:1
diethyl ether/toluene/ethanol	2:1:1
butanol/diethyl ether	2:5
aromatic	
toluene/methylene chloride	1:1 or excess toluene
toluene/acetone	1:1 or excess toluene
toluene/EtOH or MeOH	1:1 or excess toluene
toluene/acetonitrile	1:1 or excess toluene
toluene/chloroform	1:1 or excess toluene
water	
water/propylene glycol	1:1
water/glycerol	4:1 to 1:4
water/(poly)ethylene glycol	4:1 to 1:4

Glassing Agents

Pure Substance

3-methylpentane	sulfuric acid	sugar (.4 M sucrose)
methylcyclopentane	phosphoric acid	triethanolamine
paraffin oil (Nujol)	ethanol	2-methyltetrahydrofuan
isopentane	isopropanol	di-n-propyl ether
methylcyclohexane	1-propanol	decalin
isooctane	1-butanol	triacetin
boric acid	glycerol	toluene

based on R. S. Drago, Physical methods for chemists, 1992

8th BRNO EFEPR SCHOOL

partially-oriented samples

alumina-silicate layered material (hectorite)

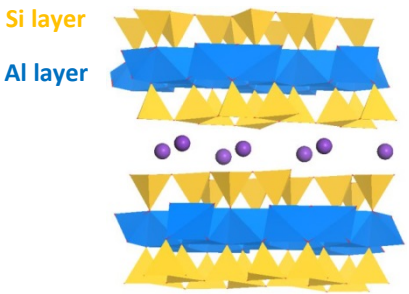

Advanced Techniques for Clay Mineral Analysis, Elsevier, 1981

EPR spectra of Cu(II) probe

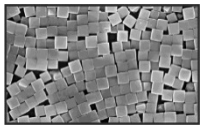

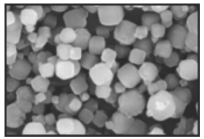

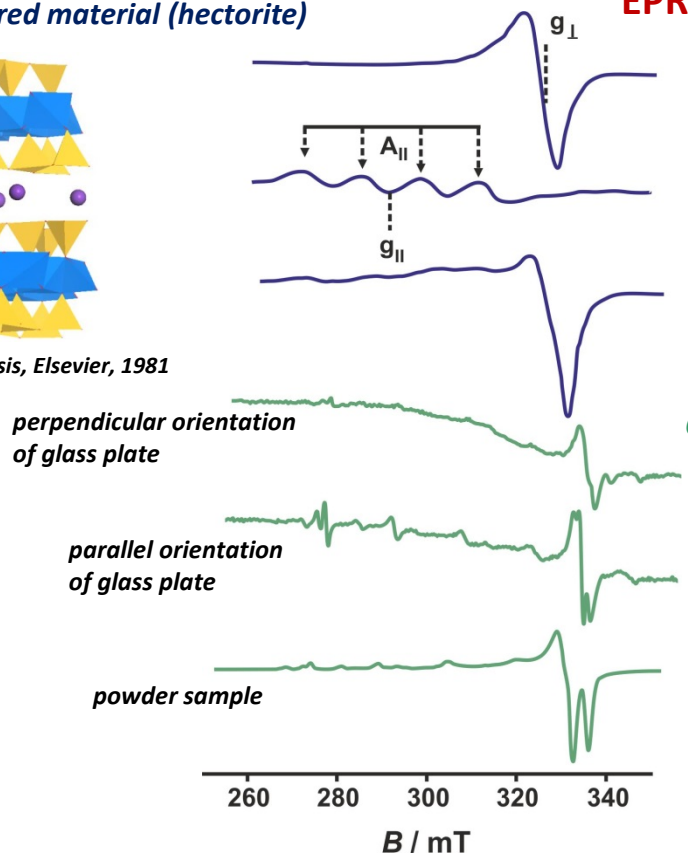

Cu-A zeolite microcrystals deposited on a glass plate

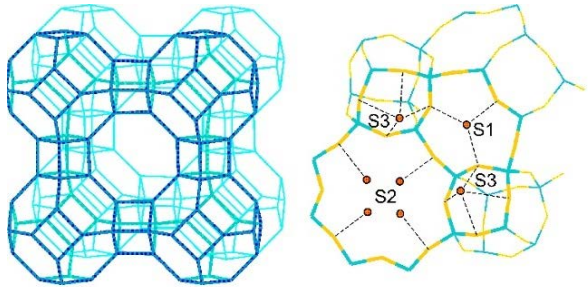

J. Phys. Chem. B, 2003, 107, 8281

more details on partially oriented powders: F. E. Mabbs, D. Collison, *Electron Paramagnetic Resonance of d Transition Metal Compounds*, Elsevier, 1992.

orientation-dependent EPR spectrum of monocrystal

reference axis system

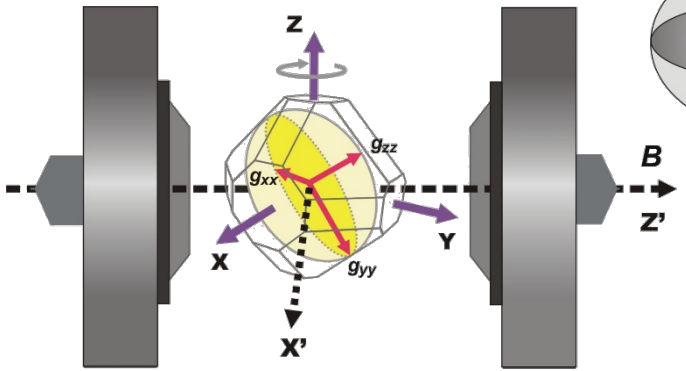

***g*-tensor elipsoide**

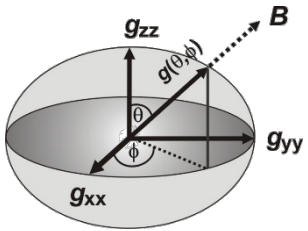

EPR measurements for a monocrystal

S = ½ , I = 0

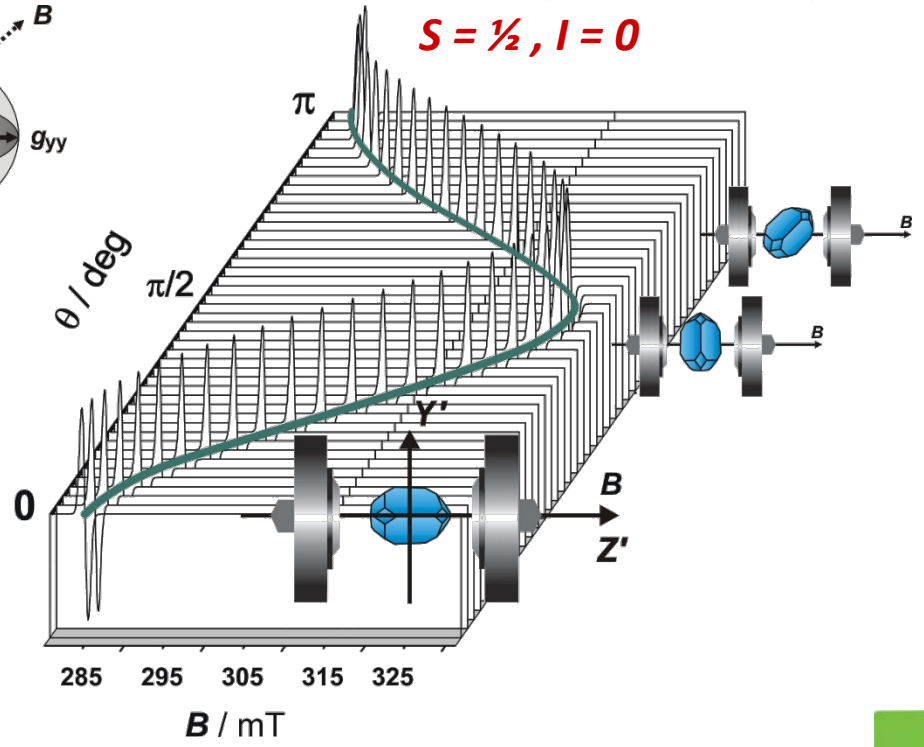

1. measure EPR spectra with respect to rotation about each crystal axe
2. find the relation $B_{rez}(\theta,\phi)$, ergo $g(\theta,\phi)$
3. fit the experimental $g(\theta,\phi)$ relationship to the theoretical equations

$$g_{eff}^2 = g_{ii}^2 \cos^2\theta + g_{jj}^2 \sin^2\theta + 2g_{ij}^2 \sin\theta\cos\theta$$

4. calculate the principal components of *g*-tensor (g_{xx}, g_{yy}, g_{zz}) – and orientation of the *g*-frame with respect to the crystal frame

angular dependency of *g* factor

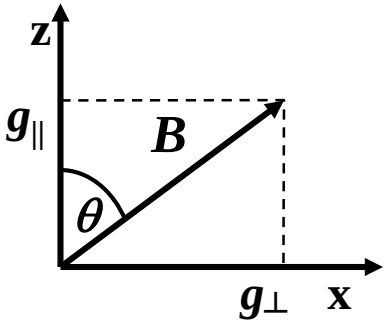

example for axial symmetry

$$H = \hbar^{-1}\mu_B[g_\perp B_x S_x + g_{\|} B_z S_z]$$

$$H = \hbar^{-1}\mu_B B[g_\perp S_x \sin\theta + g_{\|} S_z \cos\theta]$$

calculation of matrix elements H_{ij}

$$\langle\alpha|H|\alpha\rangle = 1/2\mu_B B g_{\|}\cos\theta \qquad \langle\alpha|H|\beta\rangle = 1/2\mu_B B g_\perp \sin\theta$$

$$\langle\beta|H|\beta\rangle = -1/2\mu_B B g_{\|}\cos\theta \qquad \langle\beta|H|\alpha\rangle = 1/2\mu_B B g_\perp \sin\theta$$

$$\boldsymbol{g} = \begin{vmatrix} g_\perp & & \\ & g_\perp & \\ & & g_{\|} \end{vmatrix}$$

calculation of eigenvalues of H_{ij} (E)

$$\begin{array}{c} \\ \alpha \\ \beta \end{array} \begin{array}{c} \begin{array}{cc} \alpha & \beta \end{array} \\ \begin{bmatrix} 1/2\mu_B B g_{\|}\cos\theta - E & 1/2\mu_B B g_\perp \sin\theta \\ 1/2\mu_B B g_\perp \sin\theta & -1/2\mu_B B g_{\|}\cos\theta - E \end{bmatrix} \end{array}$$

$S_x|\pm 1/2\rangle = \frac{1}{2}|\mp 1/2\rangle$

angular dependency of *g* factor

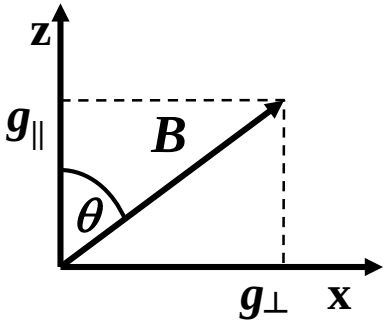

	α	β
α	$1/2\mu_B B g_{||}\cos\theta - E$	$1/2\mu_B B g_\perp \sin\theta$
β	$1/2\mu_B B g_\perp \sin\theta$	$-1/2\mu_B B g_{||}\cos\theta - E$

$$(1/2\mu_B B g_{||}\cos\theta - E)(-1/2\mu_B B g_{||}\cos\theta - E) - (1/2\mu_B B g_\perp \sin\theta)^2 = 0$$

$$E_{1,2} = \pm 1/2\mu_B B(g_{||}^2\cos^2\theta + g_\perp^2 \sin^2\theta)^{0.5}$$

$$h\nu = E_2 - E_1 = \mu_B B(g_{||}^2\cos^2\theta + g_\perp^2 \sin^2\theta)^{0.5}$$

$$h\nu = \mu_B B\, g(\theta)$$

$$g(\theta) = (g_{||}^2\cos^2\theta + g_\perp^2 \sin^2\theta)^{0.5}$$

for $g_{||} = g_\perp = g$ (isotropic system)

$$g(\theta) = g\underbrace{(\cos^2\theta + \sin^2\theta)^{0.5}}_{=1} = g$$

➡ *angular dependency vanishes*

8th BRNO EFEPR SCHOOL

angular dependency of *g* factor

rhombic symmetry

$$g = \begin{vmatrix} g_{xx} & & \\ & g_{yy} & \\ & & g_{zz} \end{vmatrix}$$

$S = 1/2 \qquad I = 0$

reference frame

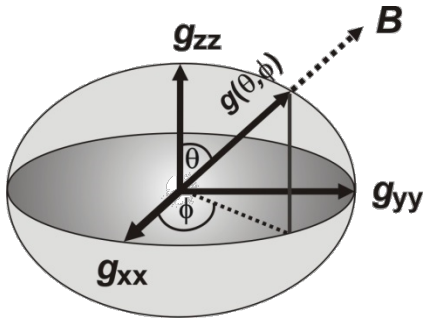

anisotropy of Zeeman interaction

$$B_{res} = \frac{h\nu_0}{g(\theta,\varphi)\mu_B}$$

$$g = \left[\left(g_{xx}^2 \cos^2\varphi + g_{yy}^2 \sin^2\varphi\right)\sin^2\theta + g_{zz}^2 \cos^2\theta\right]^{1/2}$$

randomly oriented systems

powder and frozen solution patterns

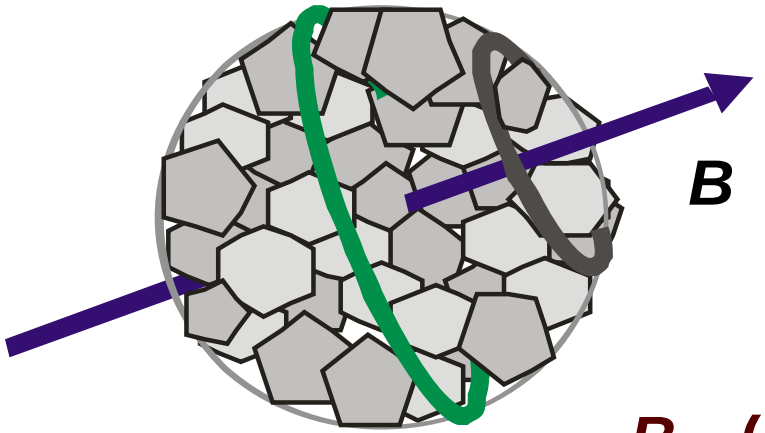

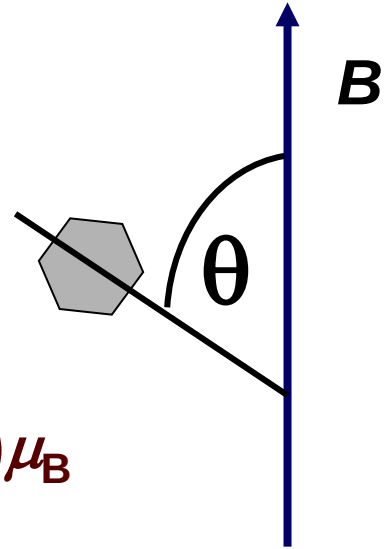

$$B_{res}(\theta) = h\nu / g(\theta)\mu_B$$

fraction of crystallites oriented within the solid angle θ and $\theta + d\theta$ with respect to the magnetic field B

randomly oriented systems

$$B_{res} = \frac{h\nu_0}{g(\theta,\varphi)\mu_B}$$

g-anisotropy induces angular dependency of EPR signal

solid angle (Ω)
and
element of area (d*A*)
on the surface of a sphere

$$\Omega = A/r^2$$

$$d\Omega = \frac{2\pi r^2 \sin\theta d\theta}{r^2} = 2\pi \sin\theta d\theta$$

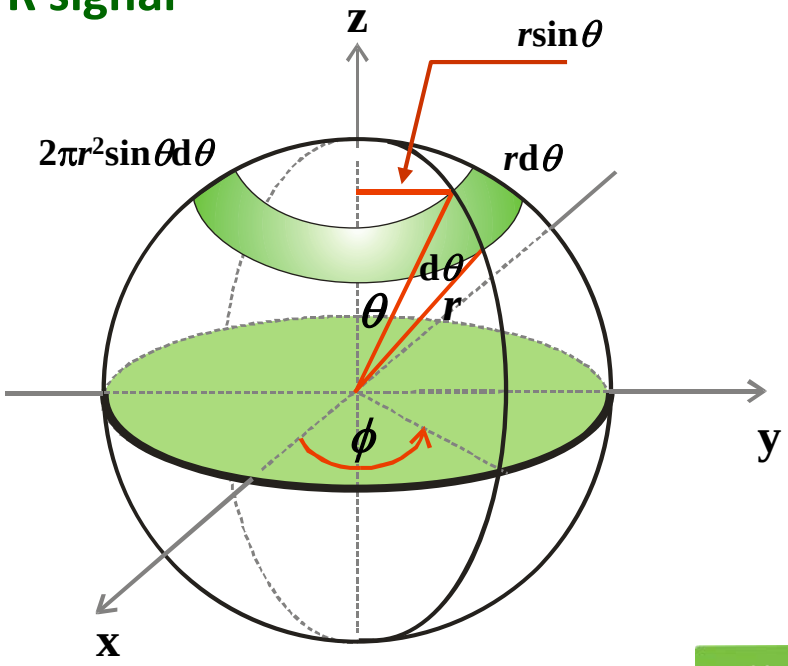

John A. Weil, James R. Bolton, Electron Paramagnetic Resonance: Elementary Theory and Practical Applications, 2007 John Wiley & Sons, Inc.

angular dependency for axial symmetry

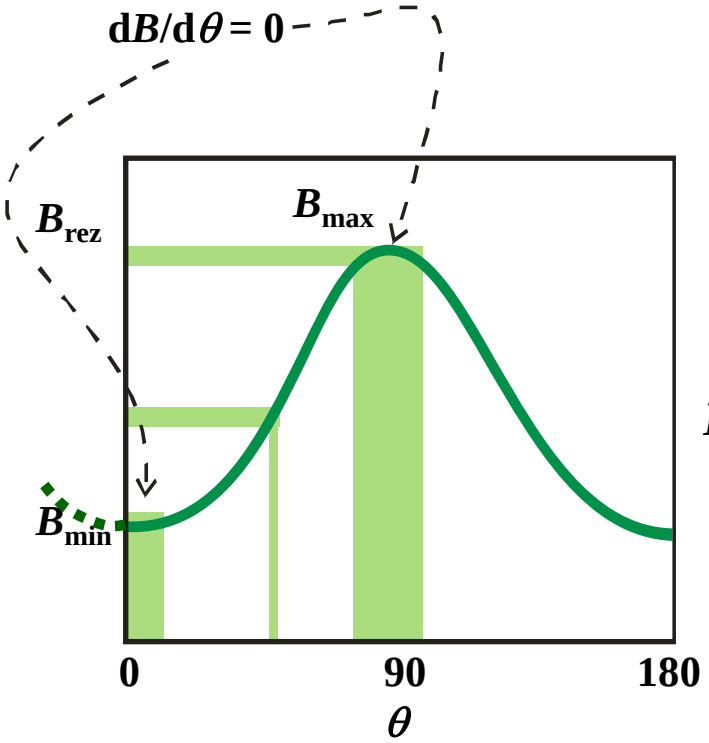

$$B = h\nu/g(\theta)\mu_B$$

$$= [g_\perp^2 \sin^2\theta + g_\parallel^2 \cos^2\theta]^{-0.5} h\nu/\mu_B$$

$$= [g_\perp^2 - (g_\perp^2 - g_\parallel^2)\cos^2\theta]^{-0.5} h\nu/\mu_B$$

bigger anisotropy - greater span of magnetic resonance field

$$P(\theta)d\theta = d\Omega/4\pi = 1/2 \sin\theta\, d\theta \sim P(B)dB$$

probability of resonance between B and B+dB

$$P(B) = 1/2C \frac{\sin\theta}{dB/d\theta}$$

fraction of crystallites with orientation within θ and θ+dθ with respect to B

$$P(B) = C/2(h\nu/\mu_B)^2 \frac{1}{B^3 \left|(g_\perp^2 - g_\parallel^2)\cos\theta\right|}$$

angular dependency for axial symmetry

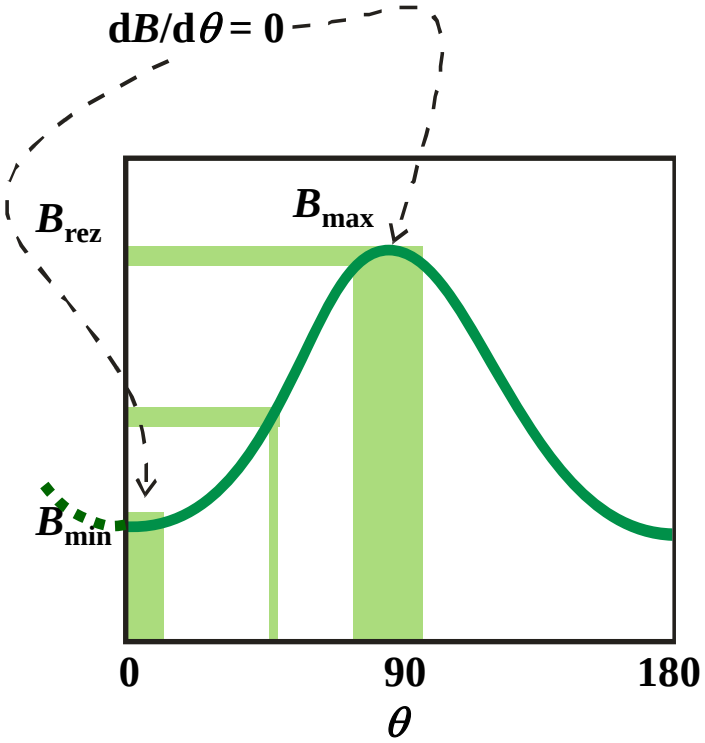

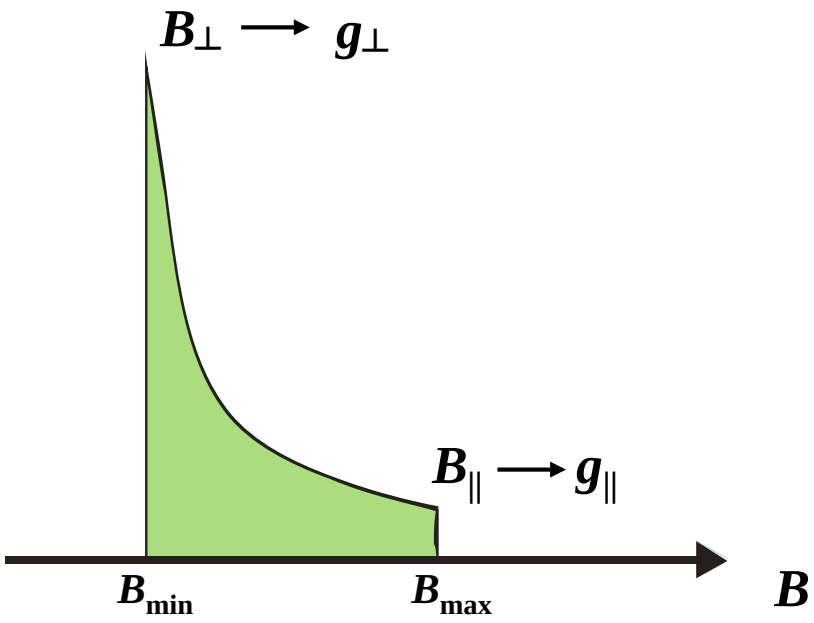

$$P(B) = C/2(h\nu/\mu_B)^2 \frac{1}{B^3 \left| (g_\perp^2 - g_\parallel^2)\cos\theta \right|}$$

absorption profiles for axial and rhombic symmetry

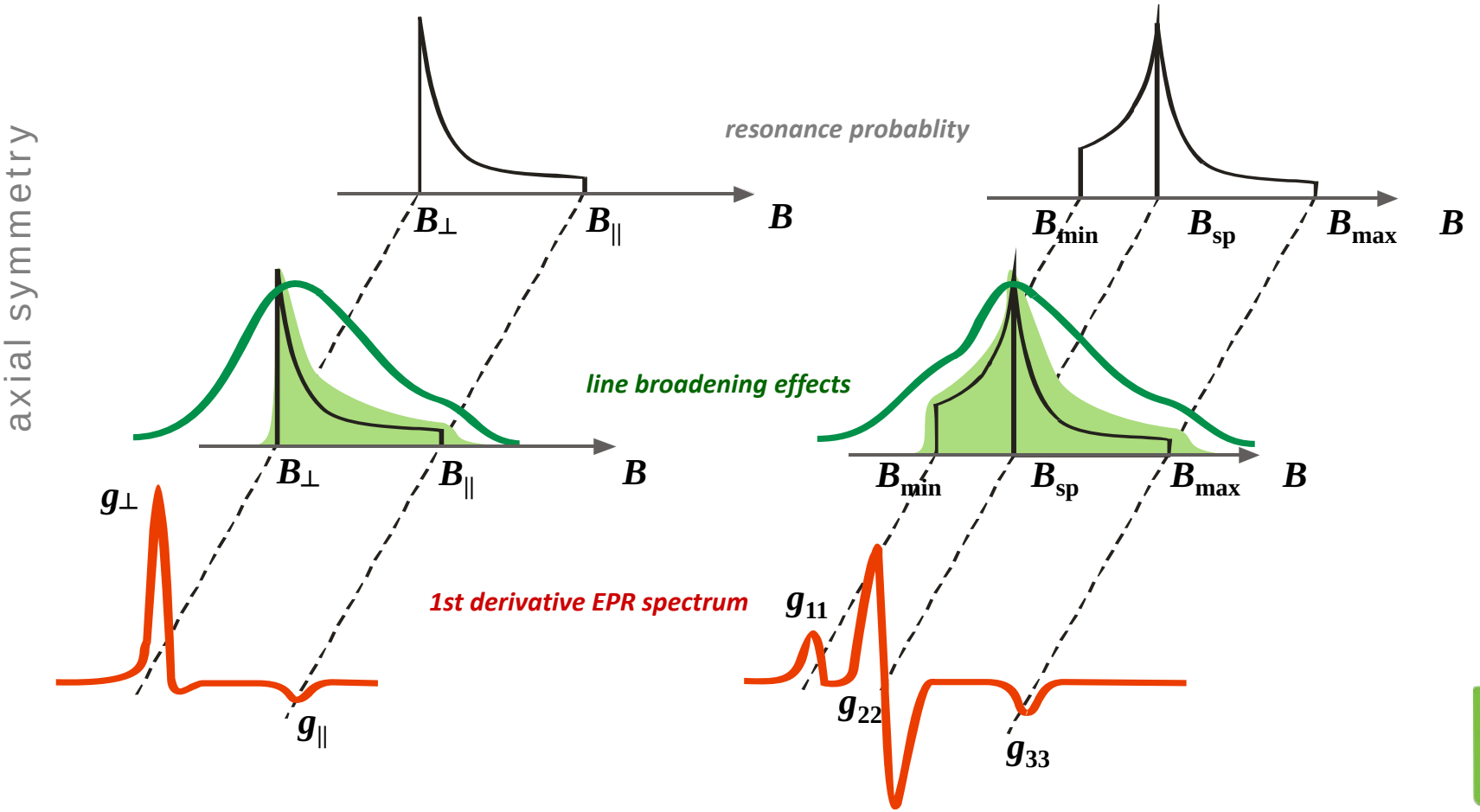

linewidth effects

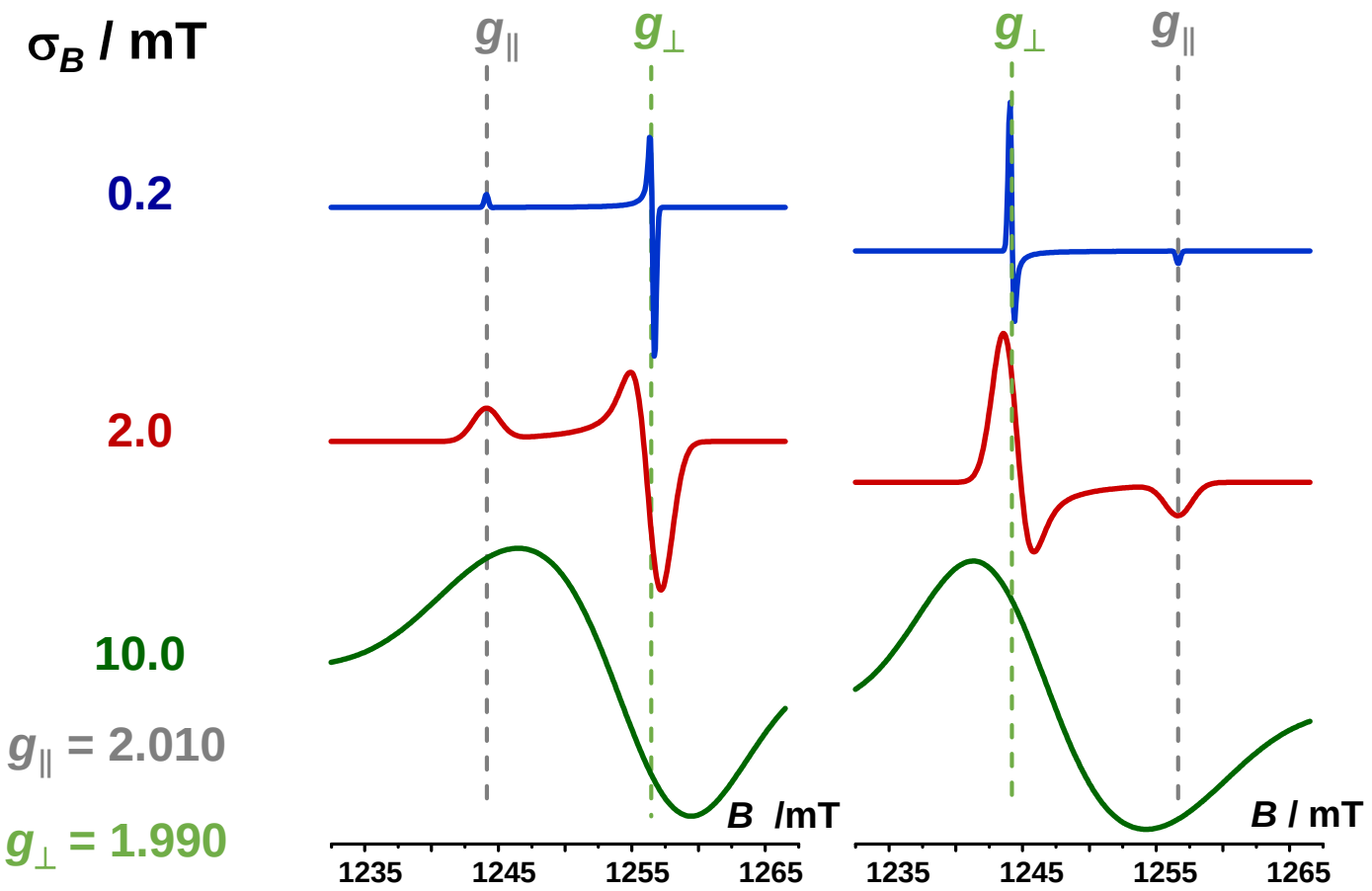

$g_{\parallel}$ = 1.990

$g_{\perp}$ = 2.010

Q-band
ν = 35.00 GHz

effect of anisotropy in *g*-values

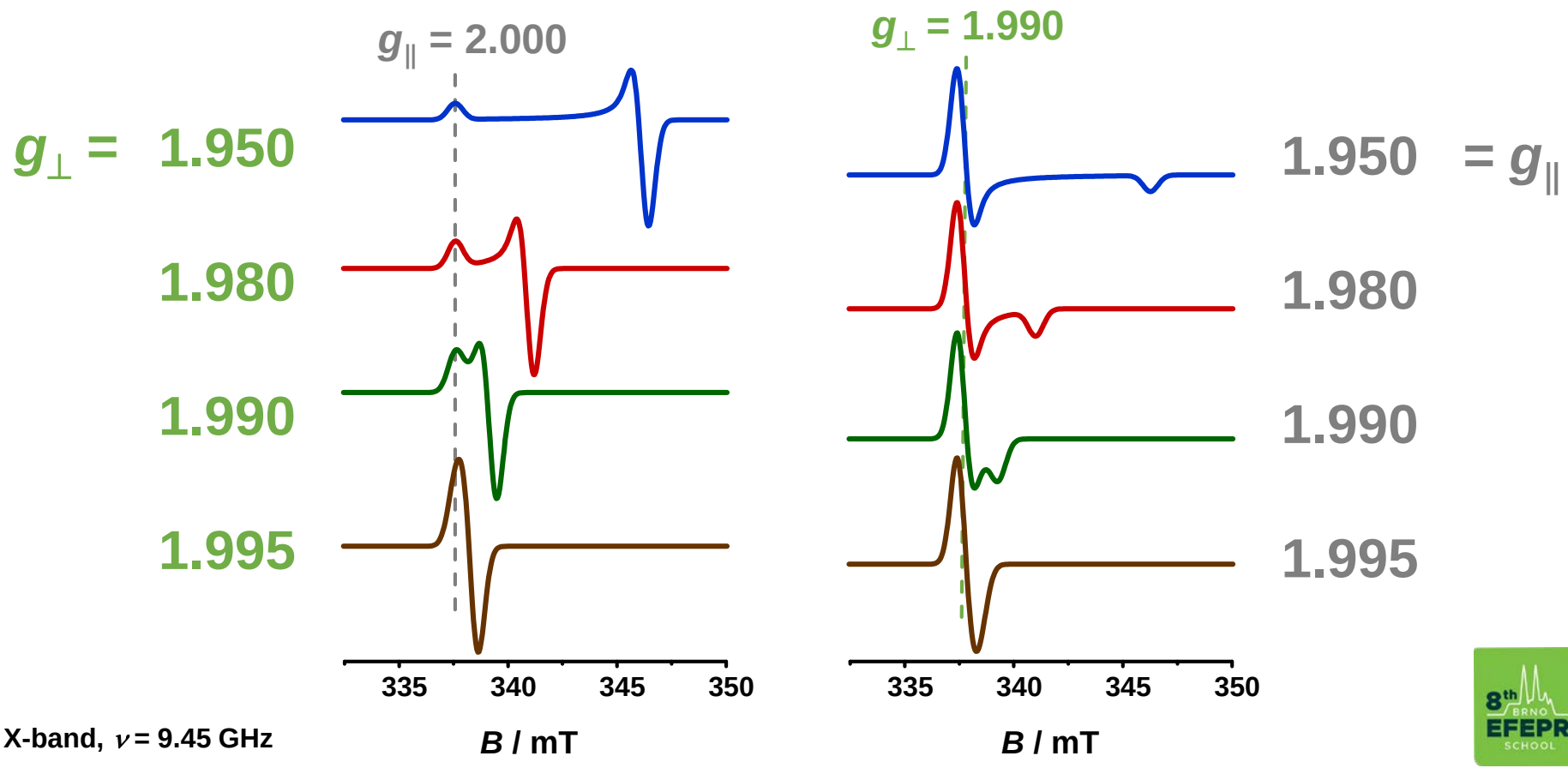

X-band, ν = 9.45 GHz

effect of anisotropy in *g*-values

Mn-doped CdSe

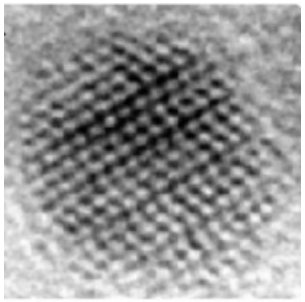

8 nm

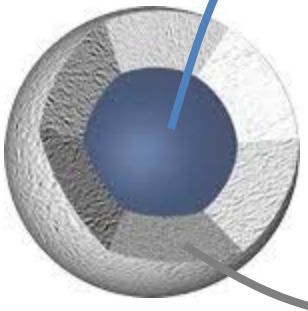

core-shell structure

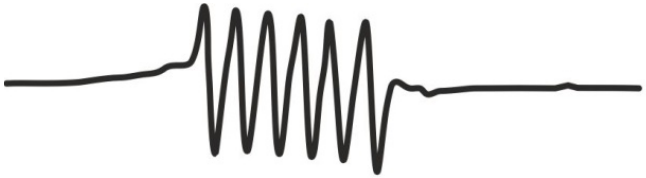

54 GHz

g_{core} = 2.004
a_{core} = 187 MHz

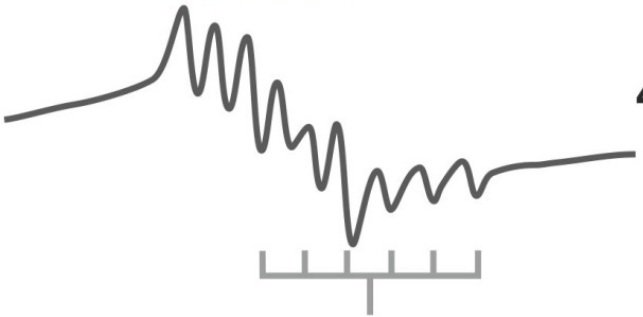

406.4 GHz

T = 11K

g_{shell} = 2.001
a_{shell} = 255 MHz

Spectra from: Z. Wang, W. Zheng, J. van Tol, N.S. Dalal, G.F. Strouse
Chem. Phys. Lett. 2012, 524, 73-77

„road maps”

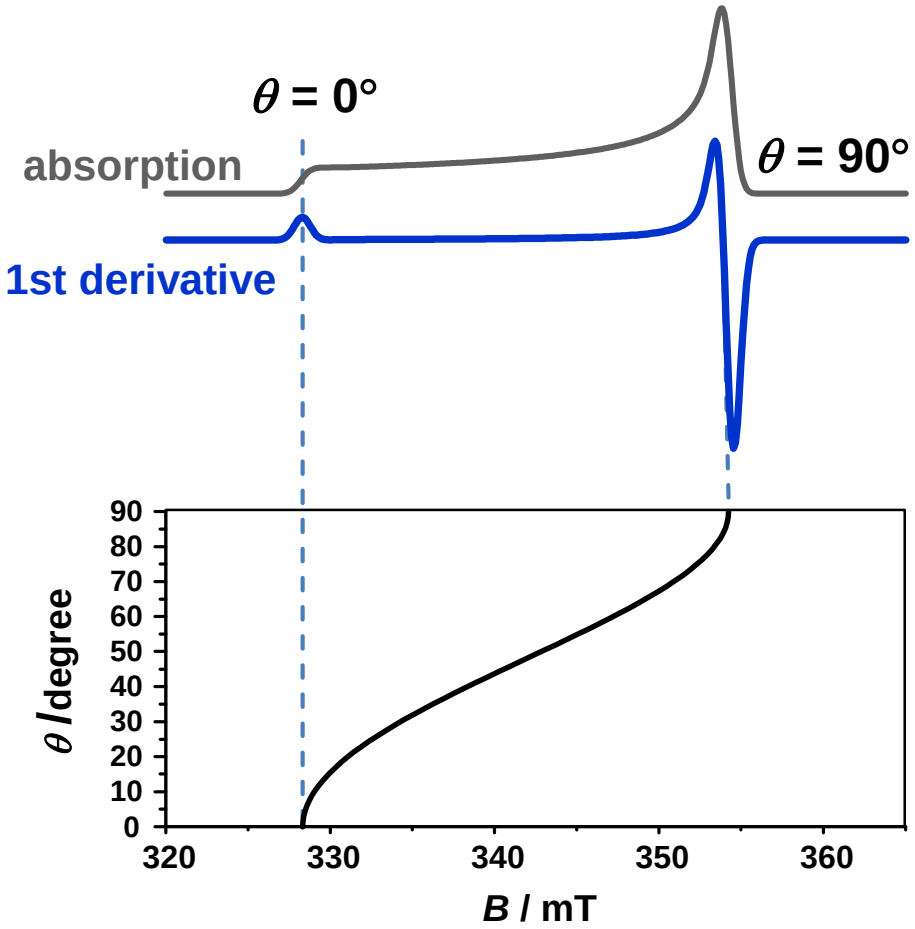

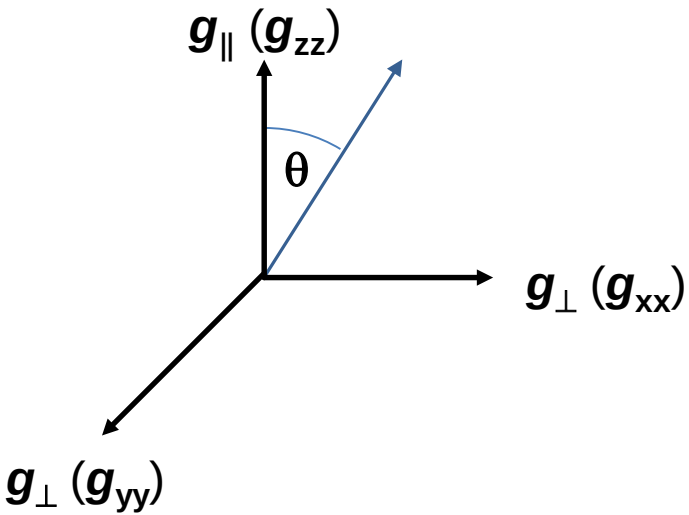

$$\theta = cos^{-1}\sqrt{\frac{g_{\theta}^2 - g_{\perp}^2}{g_{\parallel}^2 - g_{\perp}^2}}$$

resonant field B_{res} of powder sample

resonance lines in the powder EPR spectrum are coincident with the stationary points of the plot of angular dependency of *B*

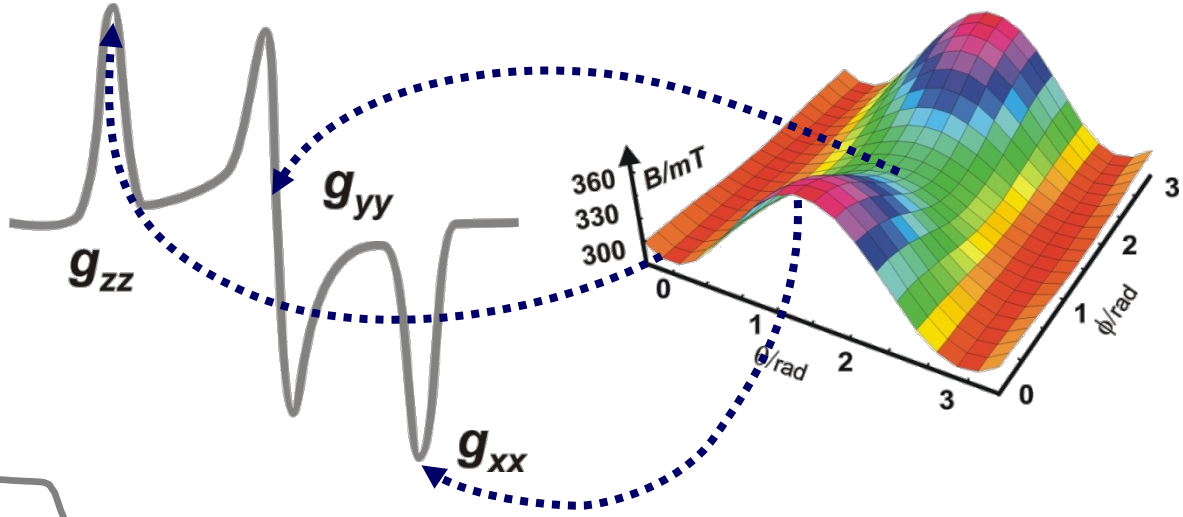

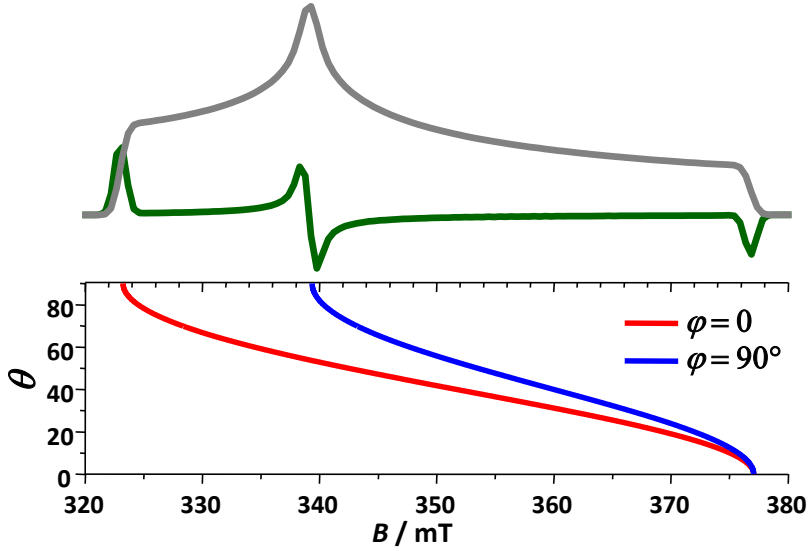

$$\frac{\partial B(\theta,\varphi)}{\partial \theta} = 0 \quad \theta = 0 \rightarrow g_{zz}$$

$$\theta = 90°, \varphi = 0° \rightarrow g_{xx}$$

$$\frac{\partial B(\theta,\varphi)}{\partial \varphi} = 0 \quad \theta = \varphi = 90° \rightarrow g_{yy}$$

8th BRNO EFEPR SCHOOL

symmetry – EPR spectrum relationship

simplest EPR symmetry

isotropic

axial

rhombic

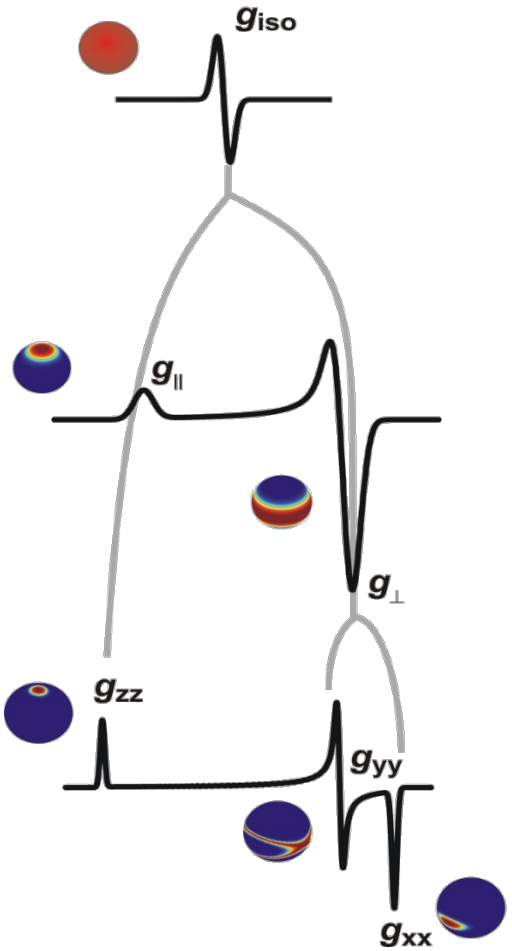

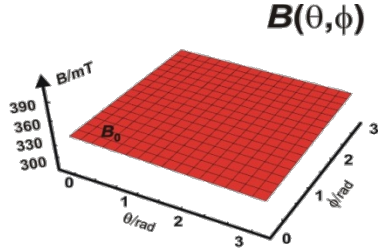

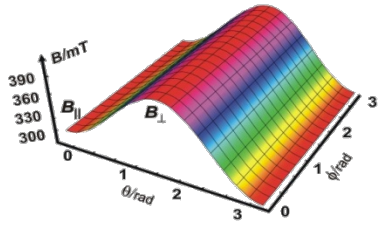

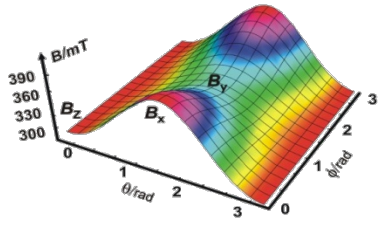

resonant magnetic field

8th BRNO EFEPR SCHOOL

anisotropy of *g*- and *A*-tensors

$$g = \begin{vmatrix} g_{xx} & & \\ & g_{yy} & \\ & & g_{zz} \end{vmatrix} \qquad A = \begin{vmatrix} A_{xx} & & \\ & A_{yy} & \\ & & A_{zz} \end{vmatrix}$$

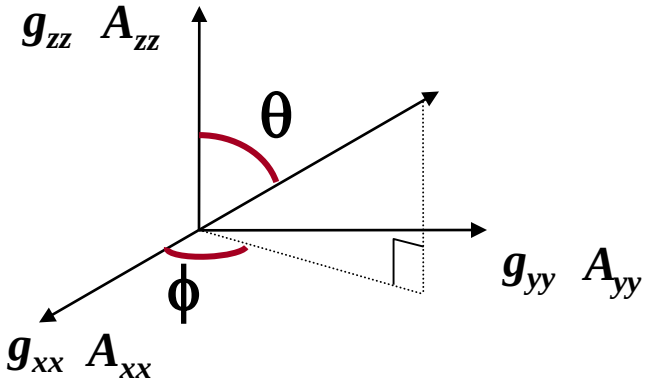

anisotropy of hyperfine interaction

$S = 1/2 \quad I \neq 0$

$$B_{res} = \frac{h\nu_0}{g\mu_B} - \frac{Km}{g\mu_B}$$

$$gK = \left[\left(g_{xx}^2 A_{xx}^2 \cos^2\phi + g_{yy}^2 A_{yy}^2 \sin^2\phi\right)\sin^2\theta + g_{zz}^2 A_{zz}^2 \cos^2\theta\right]^{\frac{1}{2}}$$

8th BRNO EFEPR SCHOOL

anisotropy of hyperfine interaction

$S = 1/2, I = 3/2$

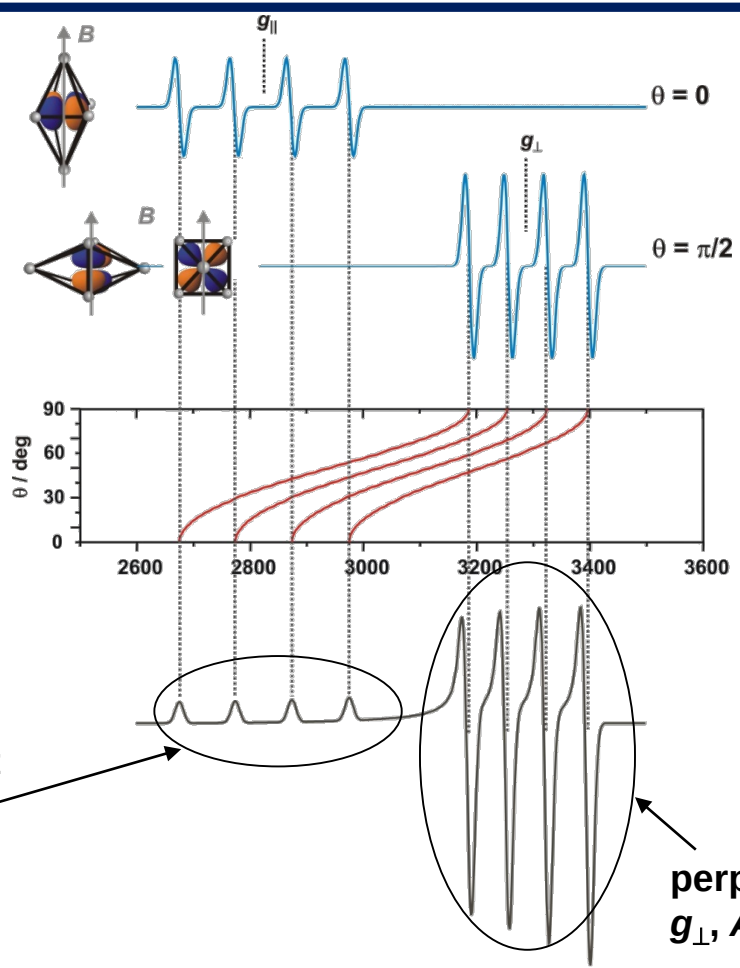

parallel orientation

perpendicular orientation

changes of the resonant field with angle θ

polioriented system
„powder spectrum"

„parallel" component
$g_{\parallel}$, $A_{\parallel}$

perpendicular component
$g_{\perp}$, $A_{\perp}$

point symmetry vs. EPR symmetry

Crystalographic system	Bravais cell	Point symmetry	EPR symmetry	Constraints	
Triclinic	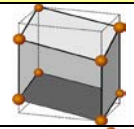	C_1, C_i	*Triclinic*	$g_{ij} \neq 0$ i $g_{xx} \neq g_{yy} \neq g_{zz}$; $A_{xx} \neq A_{yy} \neq A_{zz}$	*all non-coincident* $\alpha \neq \beta \neq \gamma \neq 0°$
Monoclinic	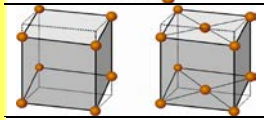	C_2, C_s, C_{2h}	*Monoclinic*	$g_{xz} = g_{yz} = g_{zx} = g_{zy} = 0$ i $g_{xx} \neq g_{yy} \neq g_{zz}$; $A_{xx} \neq A_{yy} \neq A_{zz}$	*one axis of g and one of A coincident*
Trigonal	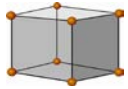	C_3, S_6	*Axial non-collinear*	As for C_2 i $g_{xx} = g_{yy} \neq g_{zz}$, $g_{xy} = -g_{yx}$; $A_{xx} = A_{yy} \neq A_{zz}$	*only g_{zz} and A_{zz} coincident*
		D_3, C_{3v}, D_{3d}	*Axial*	$g_{xy} = g_{yx} = 0$ i $g_{xx} = g_{yy} \neq g_{zz}$ $A_{xx} = A_{yy} \neq A_{zz}$	*all coincident*
Tetragonal	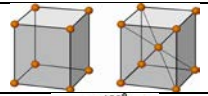	C_4, S_4, C_{4h}	*Axial non-collinear*		*as for C_3*
		D_4, C_{4v}, D_{2d}, ...	*Axial*		*as for D_3*
Hexagonal	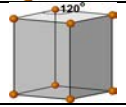	C_6, C_{3h}, C_{6h},	*Axial non-collinear*		*as for C_3*
		D_6, C_{6v}, D_{3h}, D_{6h}	*Axial*		*as for D_3*
Orthorombic	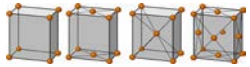	D_2, C_{2v}, D_{2h}	*Rhombic*	As for C_2 i $g_{xy} = g_{yx} = 0$	*all coincident*
Regular		T, T_h, O, T_d, O_h	*Isotropic*	As for D_3 i $g_{xx} = g_{yy} = g_{zz}$; $A_{xx} = A_{yy} = A_{zz}$	*all coincident*

F. Mabbs, D. Collison, Electron Paramagnetic Resonance of d Transition Metal Compounds, Elsevier Amsterdam, 1992

EPR symmetry

computer simulation of powder spectrum

Cu(acac)$_2$

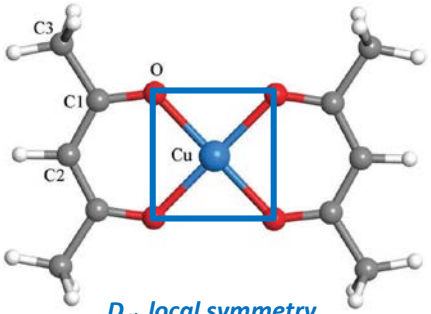

D_{4h} local symmetry

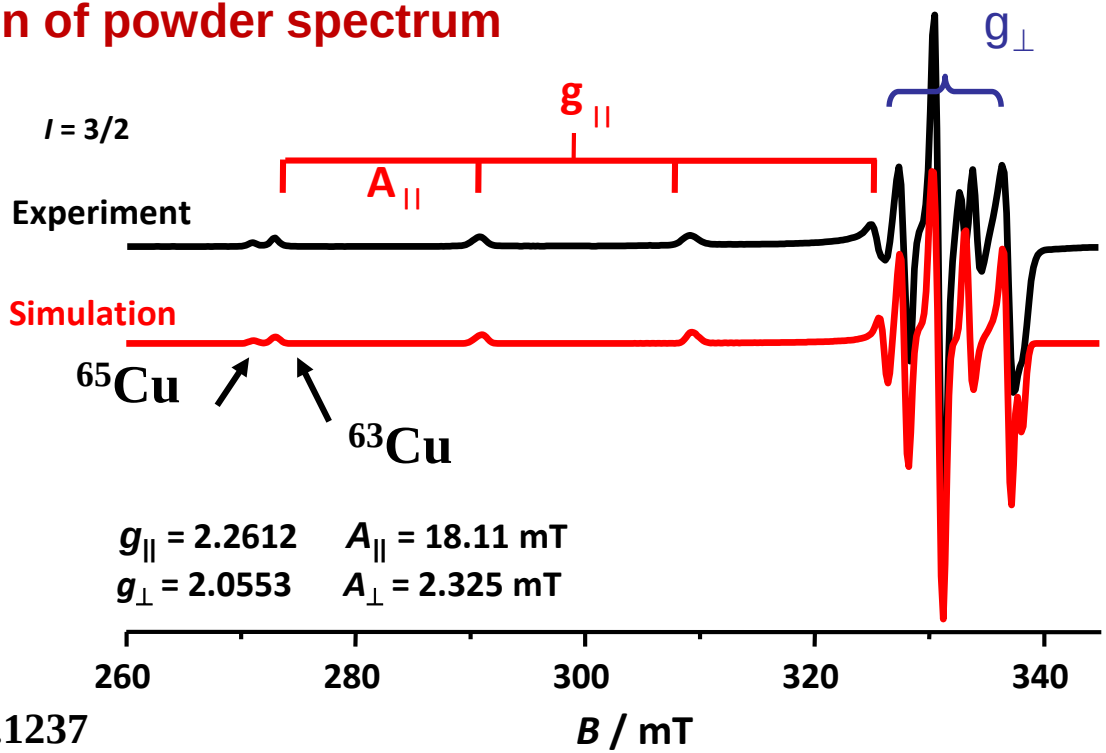

$$\langle g \rangle = \frac{1}{3}\left(2g_{\perp} + g_{//}\right) = g_{iso} = 2.1237$$

$$\langle A \rangle = \frac{1}{3}\left(2A_{\perp} + A_{//}\right) = \left|a_{iso}\right| = 7.62\ \text{mT}$$

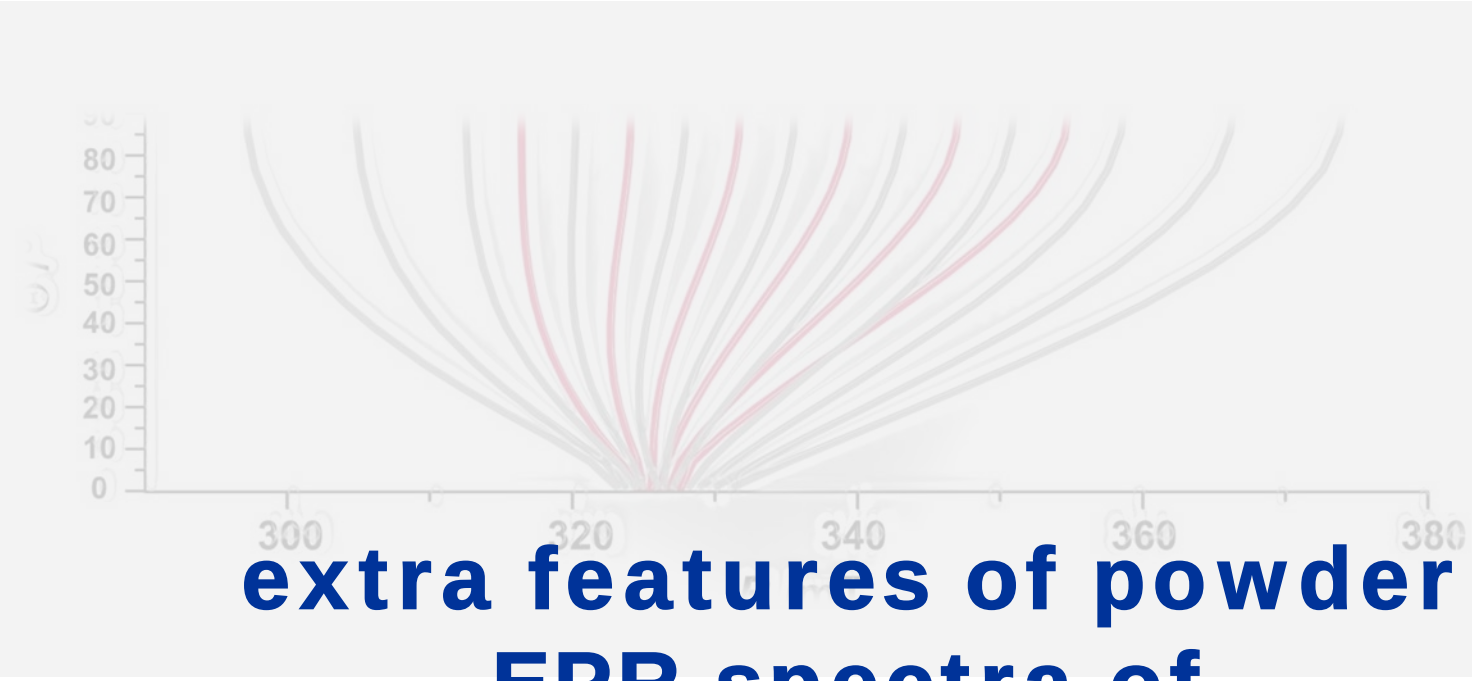

extra features of powder EPR spectra of anisotropic systems

EPR symmetry

lowering symmetry - rhombic

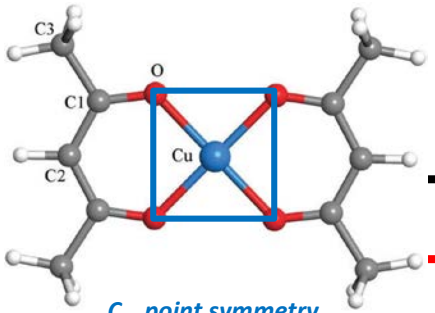

C_{2v} *point symmetry*

$I = 3/2$

z z z z x y

experimental

simulation

$g_{xx} = 2.0570$ $|A_{xx}| = 1.84$ mT

$g_{yy} = 2.0527$ $|A_{yy}| = 2.81$ mT

$g_{zz} = 2.2595$ $|A_{zz}| = 18.1$ mT

B / mT

260 280 300 320 340

8th BRNO EFEPR SCHOOL

off-axis turning points

For some combinations of the principal values of g_{ii} and A_{ii}, owing to intricate relationship of $B_{res}(\theta,\phi)$, stationary points and therefore EPR lines may arise, which do not correspond to field orientations along the principal axes of *g* and *A*

$$\left(2A_i^2 - \frac{h\nu A_i}{m}\right) < \left(\frac{g_i^2 A_i^2 - g_j^2 A_j^2}{g_i^2 - g_j^2}\right) < \left(2A_j^2 - \frac{h\nu A_j}{m}\right)$$

regular features

$\theta = 0$

$\theta = 90°, \varphi = 0°$

$\theta = \varphi = 90°$

extra, off-axis features

$\theta = 90°, \varphi = \varphi_{xy}$

$\theta = \theta_{yz}, \varphi = 90°$

$\theta = \theta_{xz}, \varphi = 0°$

I. V. Ovchinikov, V. N. Konstantinov, J. Mag. Res. 1978, 32, 179

analysis of angular effects

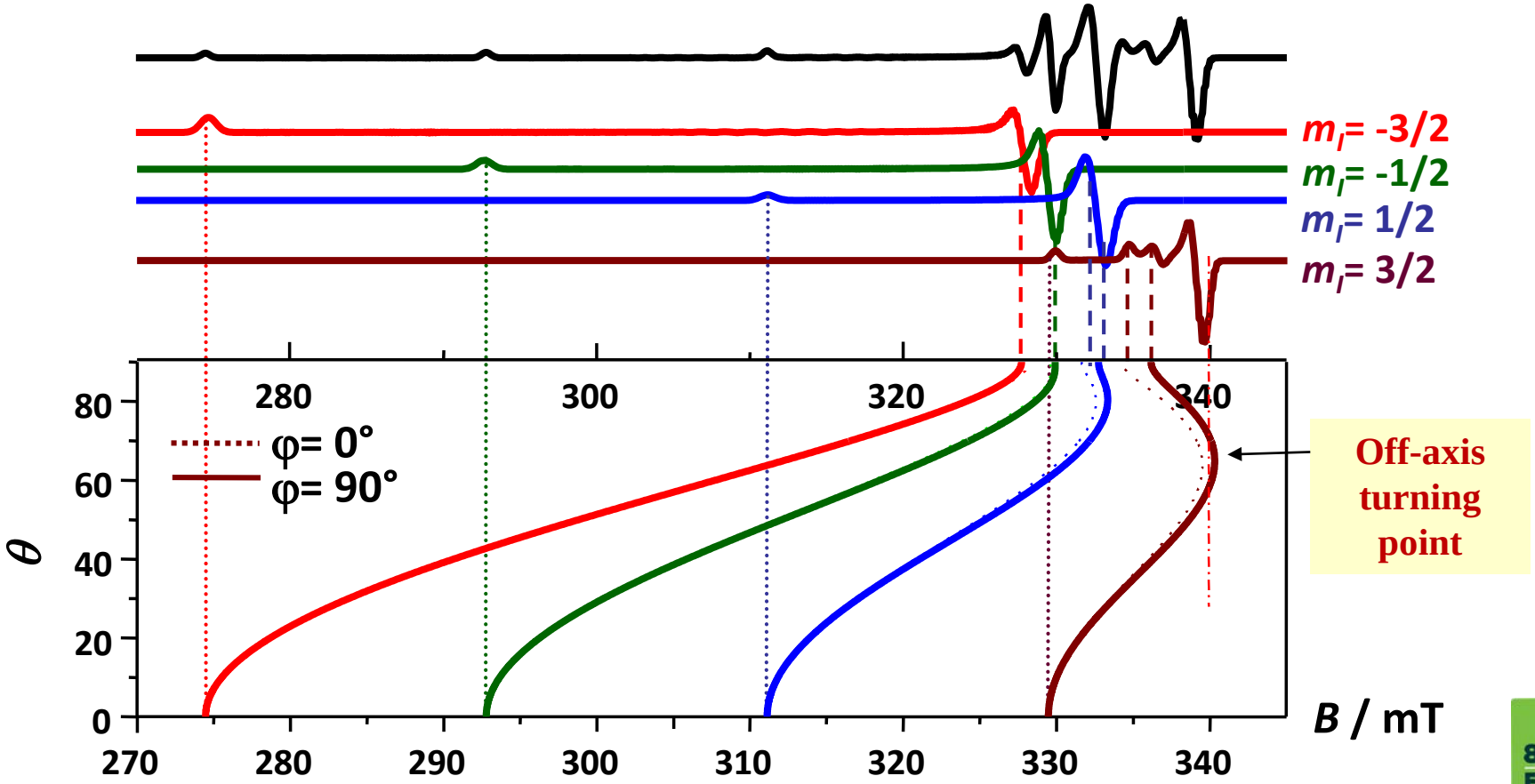

molecular complexes of Cu(II) – glass spectra

S-band
ν = 3.500 GHz
σ = 0.8 mT

X-band
ν = 9.450 GHz
σ = 2.0 mT

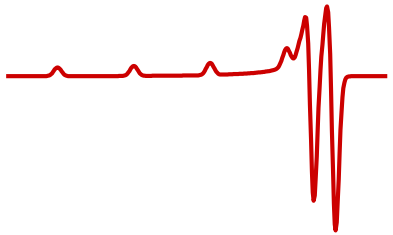

overshoot

Q-band
ν = 35.00 GHz
σ = 3.5 mT

W-band
ν = 94.50 GHz
$\sigma_{\parallel}$ = 7.0 mT
$\sigma_{\perp}$ = 9.0 mT

$g_{\parallel}$ = 2.300 $A_{\parallel}$ = 20 mT
$g_{\perp}$ = 2.050 $A_{\perp}$ = 0.5 mT

molecular complexes of Cu(II) – glass spectra

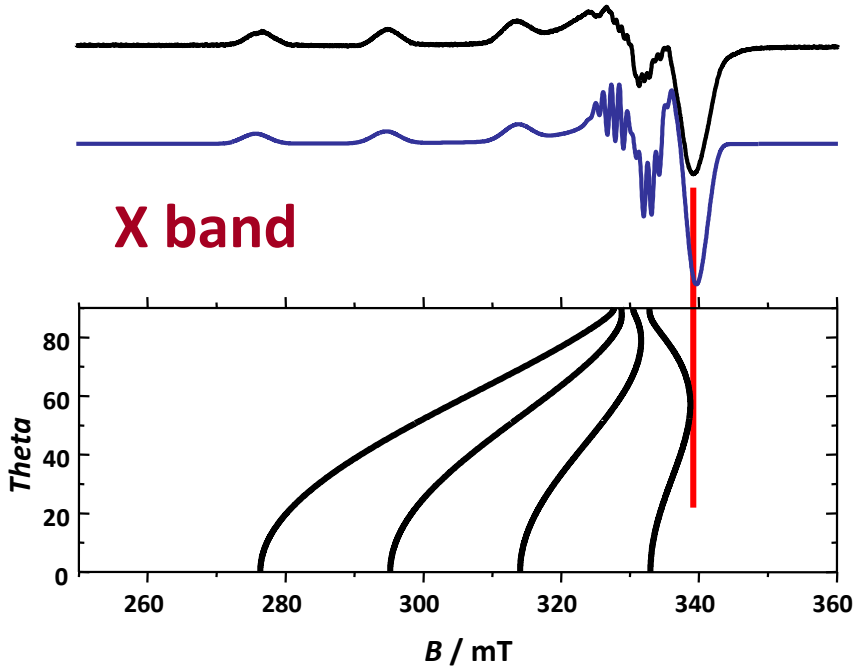

Off-axis turning point

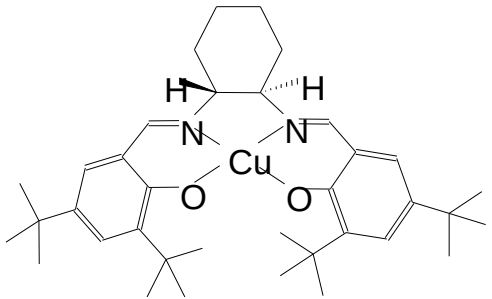

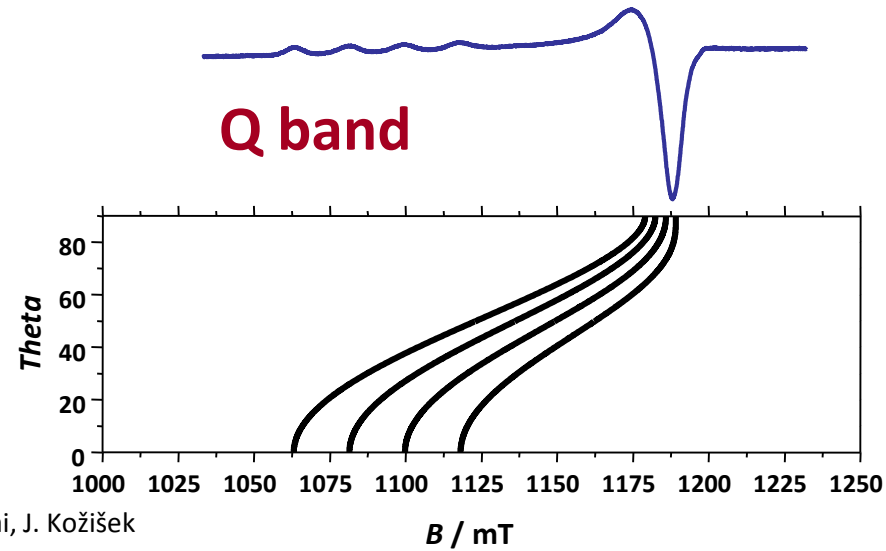

Data from: V.B. Arion, P. Rapta, J. Telser, S.S. Shova, M. Breza, K. Lušpai, J. Kožišek *Inorg. Chem. 2011, 50, 2918–2931.*

MgO superoxide surface species

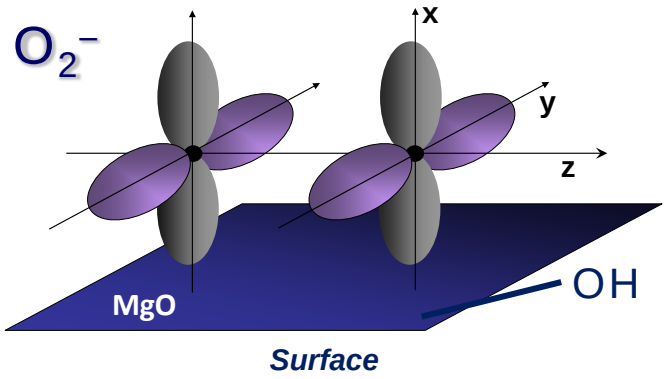

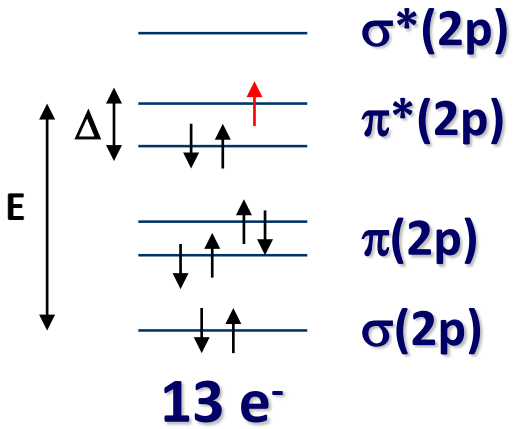

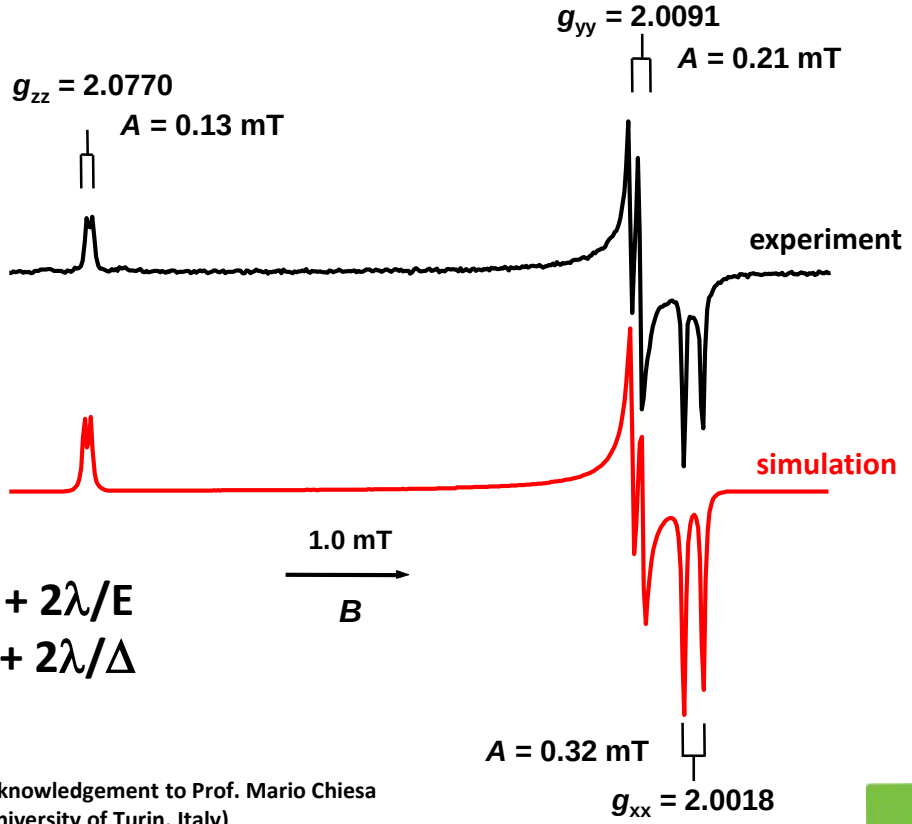

$g_{xx} \approx g_e$

$g_{yy} = g_e + 2\lambda/E$

$g_{zz} = g_e + 2\lambda/\Delta$

Acknowledgement to Prof. Mario Chiesa
(University of Turin, Italy)

Spectra taken from: M. Chiesa, E. Giamello, M. C. Paganini, Z. Sojka, D. M. Murphy
J. Chem. Phys. 2002, 116, 4266-4274

^{16}O and ^{17}O isotopomeres of O_2^-

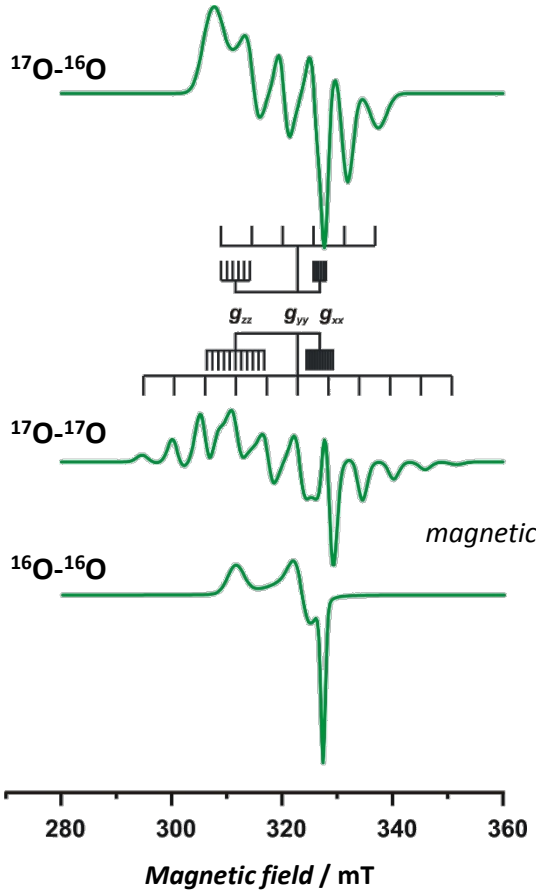

^{17}O (I = 5/2)

$P^{17\text{-}16} = 2p(1\text{-}p) = 49\%$

$N = 2 \times I + 1 = 6$

$P^{17\text{-}17} = p^2 = 31\%$

$N = 2 \times In + 1 = 11$

magnetically equivalent nuclei

$P^{16\text{-}16} = (1\text{-}p)^2 = 20\%$

$N = 2 \times I + 1 = 0$

Species	$^{16}O^{16}O$	$^{16}O^{17}O$ $^{17}O^{16}O$	$^{17}O^{17}O$
Concentration	$(1 - x)^2$	$2x(1 - x)$	x^2
Number of lines	1	6	11
Distribution of lines		5/2 3/2 1/2 -1/2 -3/2 -5/2	5 4 3 2 1 0 -1 -2 -3 -4 -5

x – ^{17}O enhancement level

simulated exemplary spectra from
Pietrzyk et al. J. Am. Chem. Soc., *133*, 19931–19943, 2011

8th BRNO EFEPR SCHOOL

^{16}O and ^{17}O isotopomeres of O_2^-

variable enrichment approach for controlling the isotopomer composition

Isotopomers of O_2^-

^{16}O-^{16}O

^{16}O-^{17}O

^{17}O-^{16}O

^{16}O-^{17}O

^{17}O-^{16}O

^{17}O-^{17}O

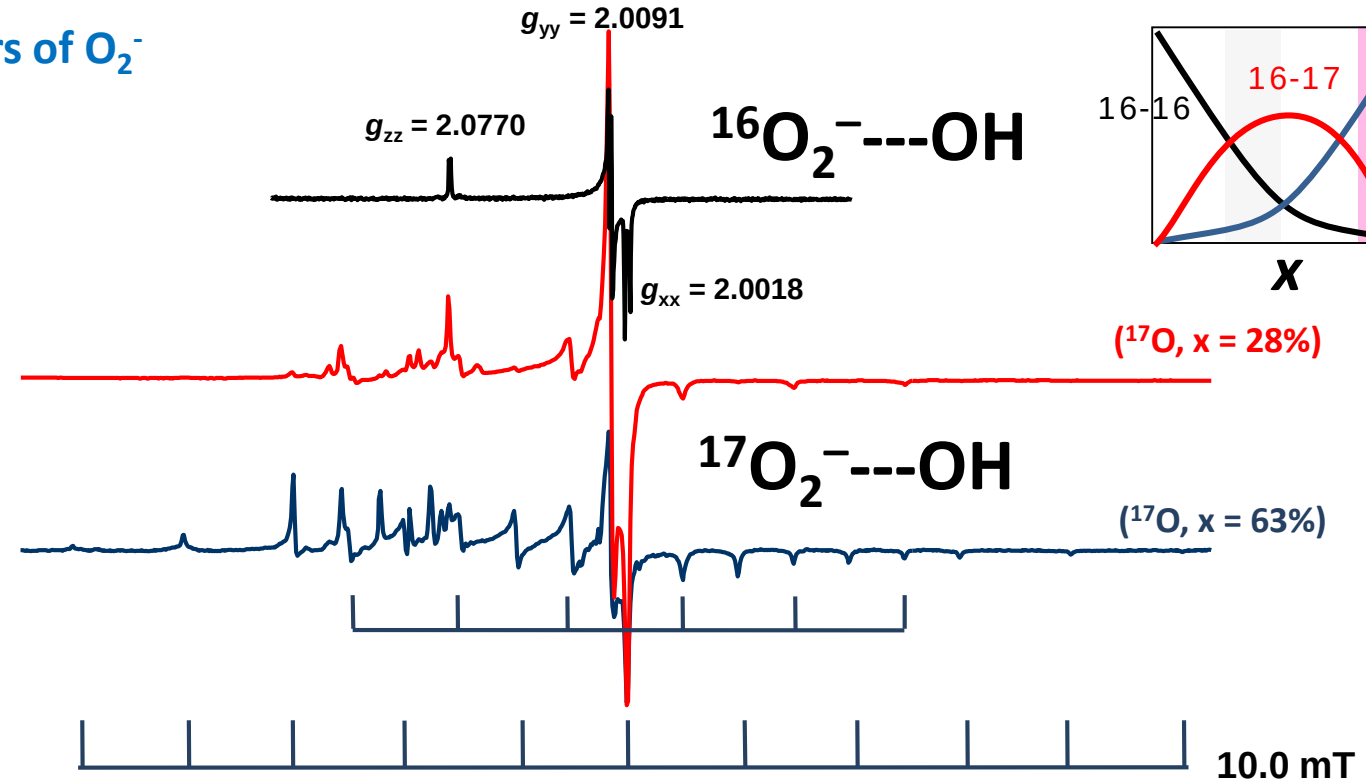

simplification of the spectra through suppression of the speciation and controlled enrichment

Acknowledgement to Prof. Mario Chiesa
(University of Turin, Italy)

Case study: J. Chem. Phys. 2002, 116, 4266-4274

8th BRNO EFEPR SCHOOL

$^{16}O^{17}O^-$ isotopomer

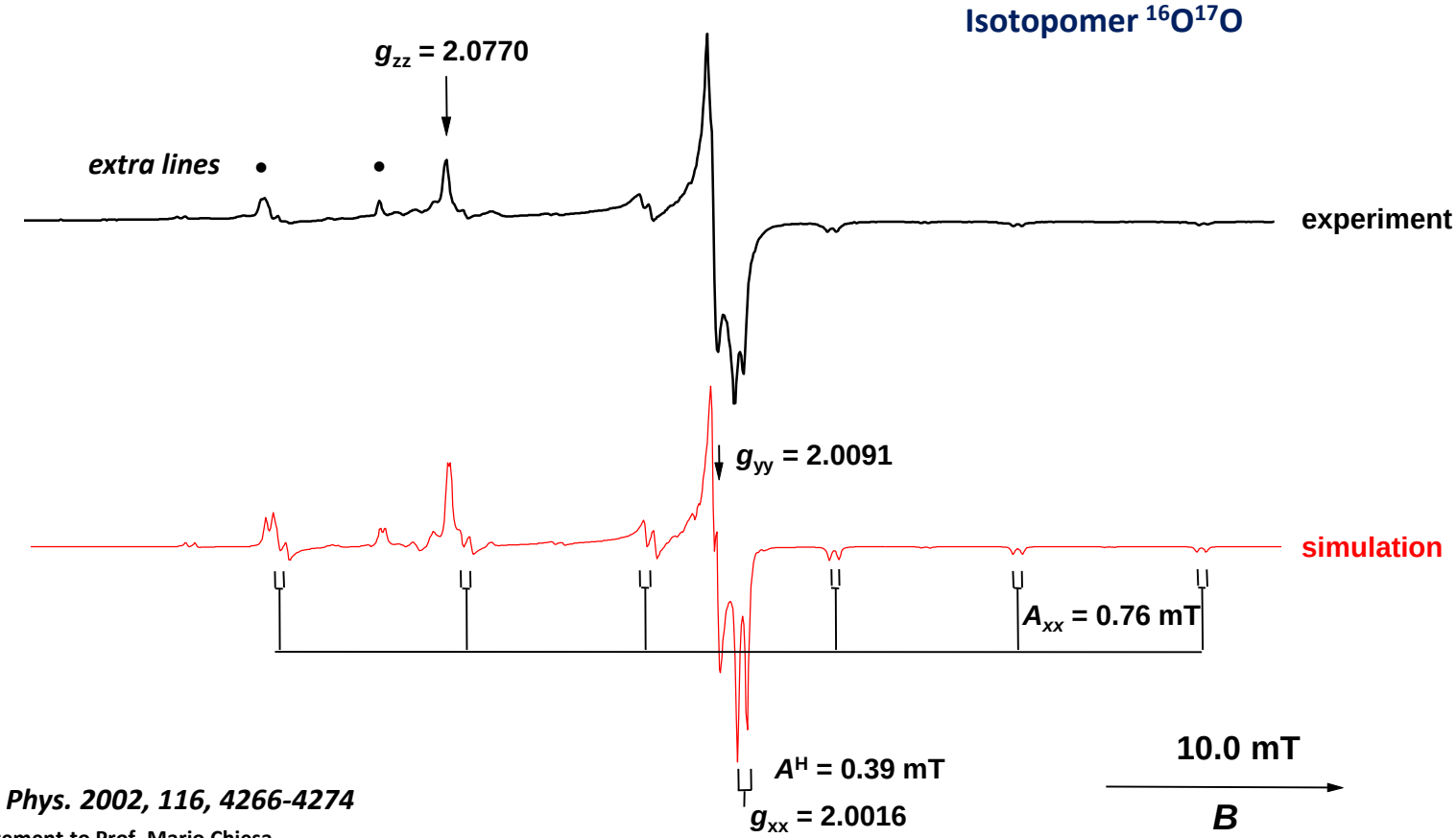

J. Chem. Phys. 2002, 116, 4266-4274

Acknowledgement to Prof. Mario Chiesa
(University of Turin, Italy)

identification of extra features

J. Chem. Phys. 2002, 116, 4266-4274

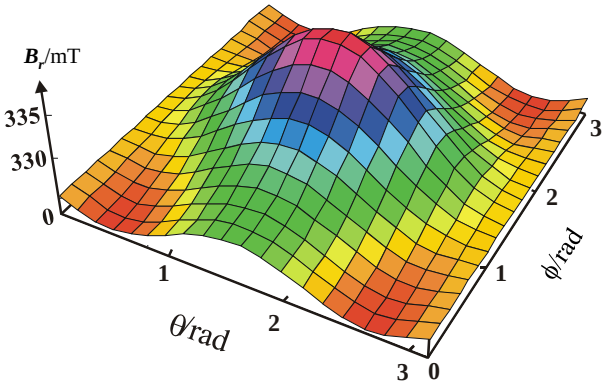

resonance field for m_I = 3/2

$$\frac{\partial B(\vartheta,\varphi)}{\partial \vartheta} = 0$$

θ=28.8°; θ=0°;

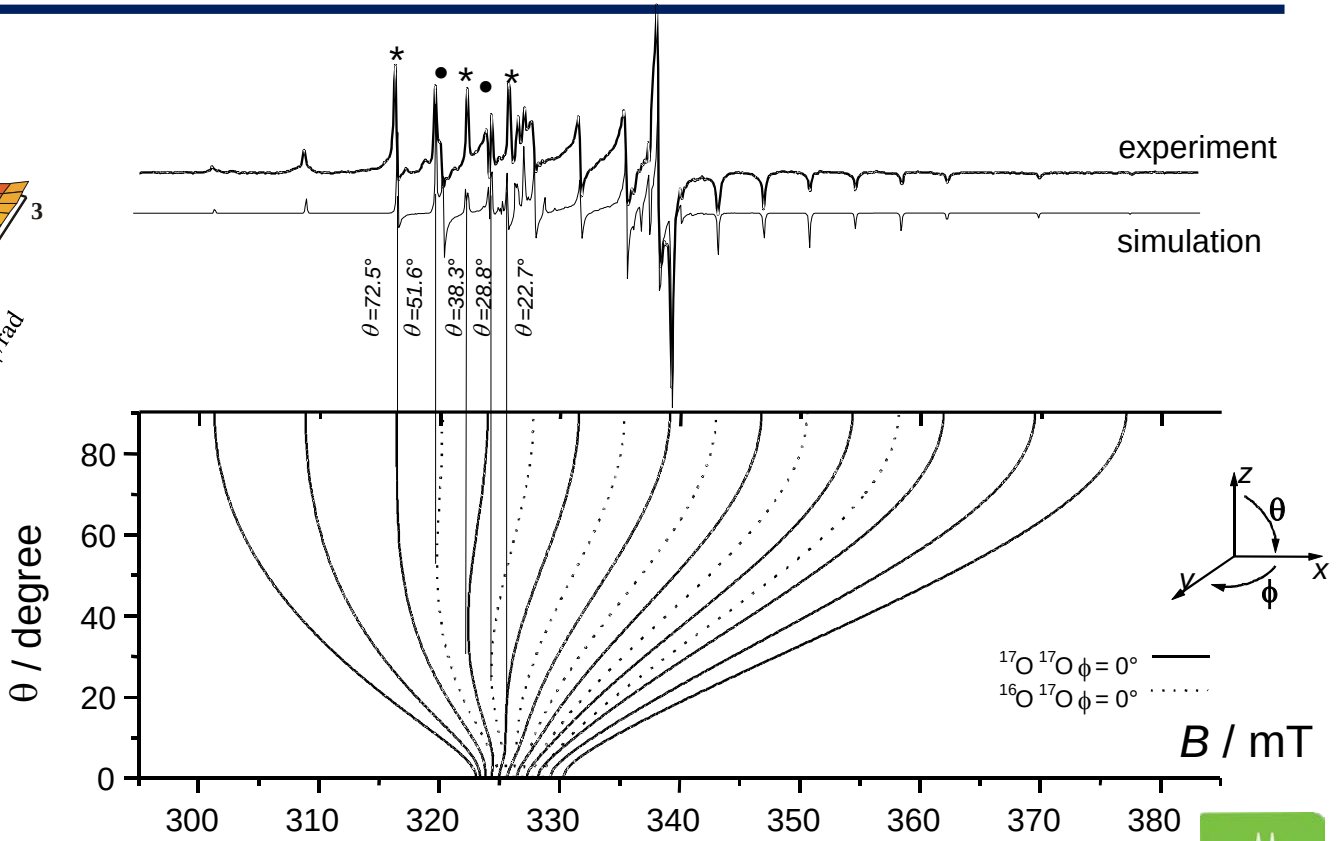

5 extra lines corresponding to additional extremes in $B_r(\theta,\phi)$ for m_I = 3, 5/2, 2, 3/2, 1

identification of extra features

$MgO–{}^{17}O{}^{17}O^{-}$ line $m_I = 5$

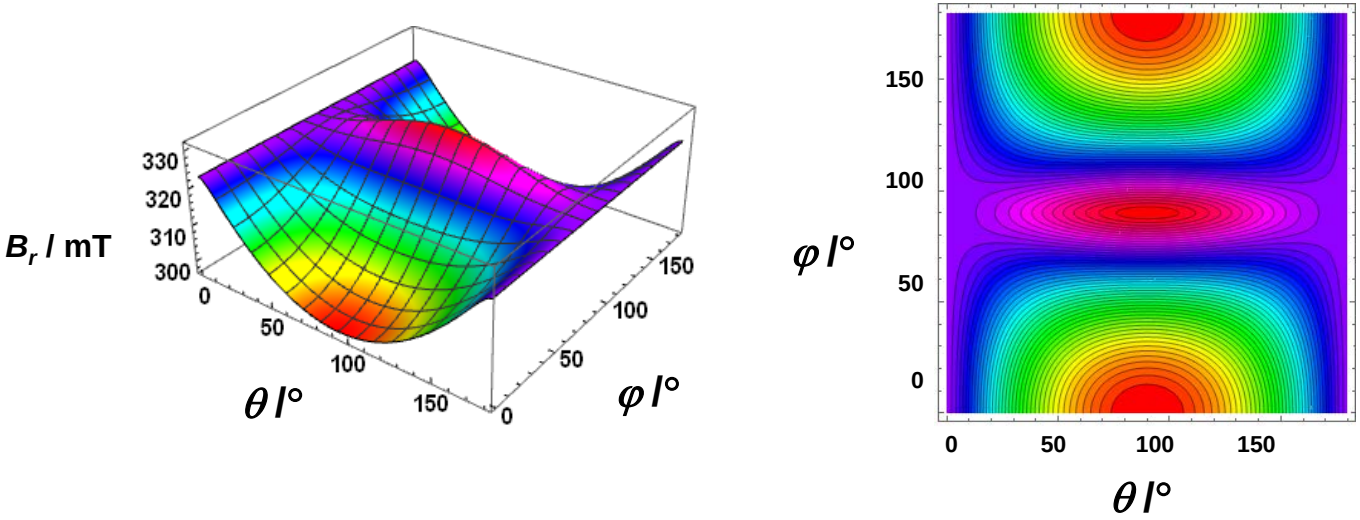

all regular resonances

identification of extra features

MgO–^{17}O^{17}O^{-}

line $m_I = 2$

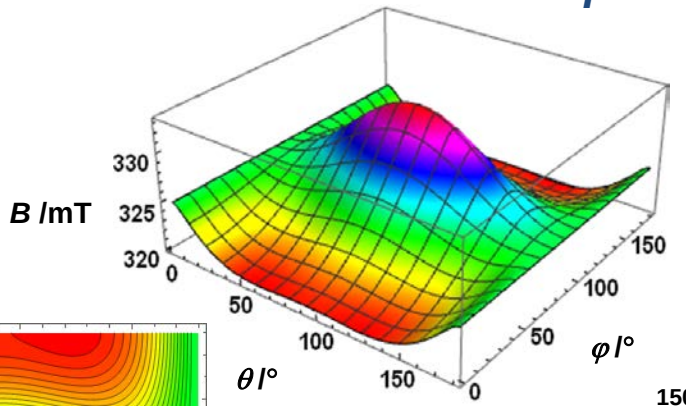

line $m_I = 1$

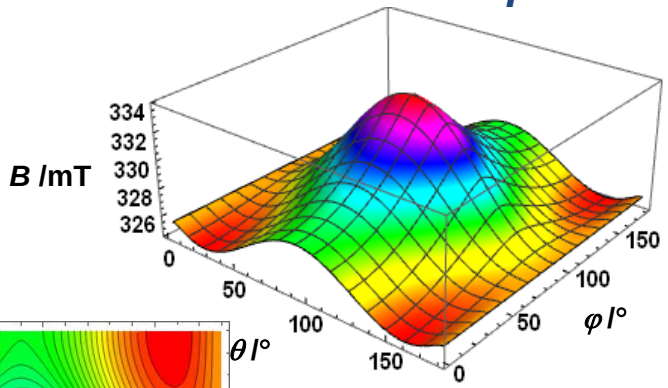

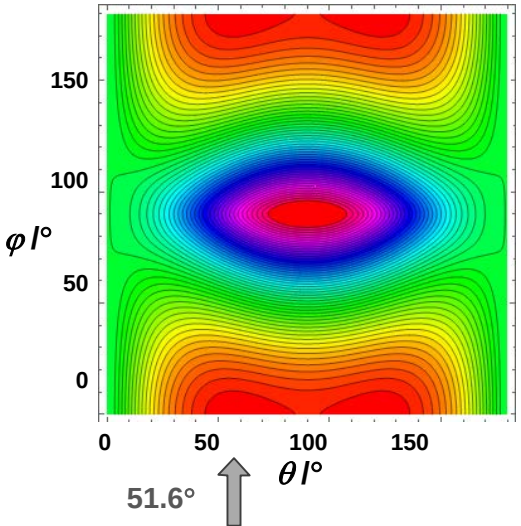

off-axis extra lines

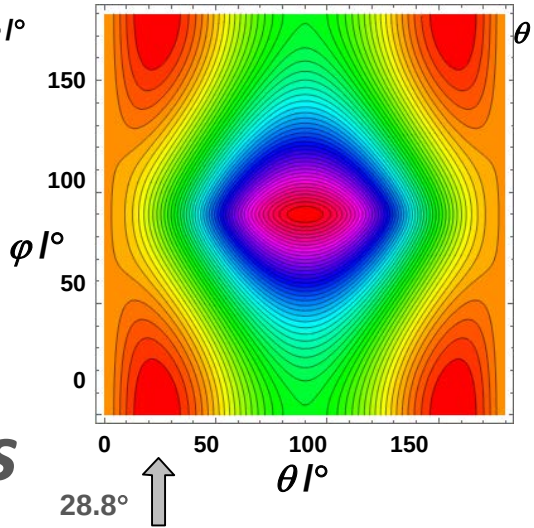

8th BRNO EFEPR SCHOOL

extra lines – what for?

using extra lines to pin down the $^{O}A_{zz}$ value

extra lines $^{O}A_{zz} = 0.83 \pm 0.20$ mT

simulation $^{O}A_{zz} = 0.73$ mT

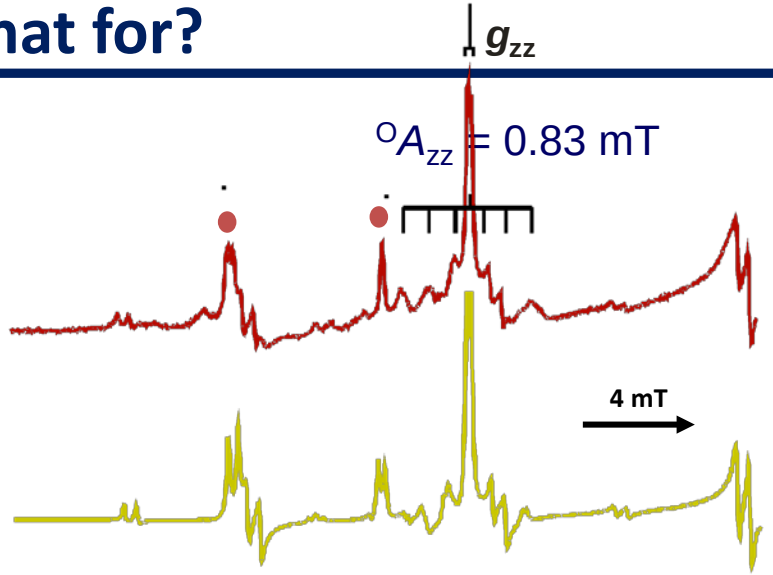

$$B_{zx}(m_I) = \frac{h\nu}{g_{zx}\beta_e}\left[1 - m_I K_{zx} - \frac{[I(I+1) - m_I^2](A'^2_{yy} + A'^2_{zz} A'^2_{xx})}{K_{zx}^2/4} - \frac{m_I^2(K_{zx}^2 - A'^2_{zz})(A'^2_{xx} - K_{zx}^2)}{2K_{zx}^2}\right]$$

$$K_{zx} = \frac{1}{4m_I}[1-(1+m_I^2\Delta_{zx})^{1/2}] \qquad \Delta_{zx} = \frac{g_{zz}^2 A'^2_{zz} - g_{xx}^2 A'^2_{xx})}{(g_{zz}^2 - g_{xx}^2)} \qquad A'_{ij} = A_{ij}/h\nu$$

$$g_{zx} = \frac{g_{zz}^2 g_{xx}^2 (A'^2_{zz} - A'^2_{xx})}{(g_{zz}^2 - g_{xx}^2)(\Delta_{zx} - K_{zx}^2)}$$

Acknowledgement to Prof. Zbigniew Sojka
(Jagiellonian University in Krakow, Poland)

8th BRNO EFEPR SCHOOL

superhyperfine and hyperfine structure $^{17}O_2^-/H^+$ on MgO

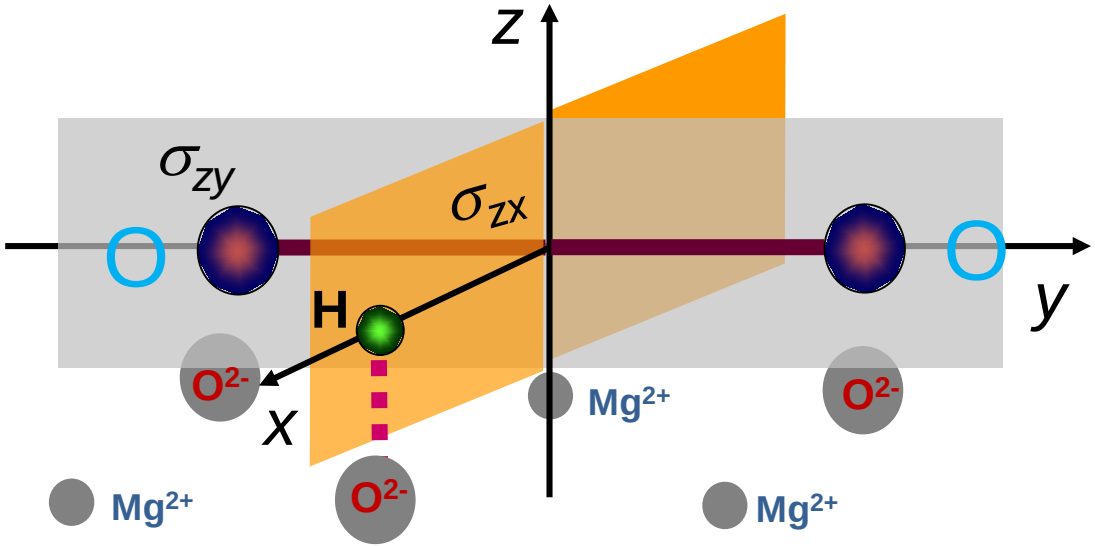

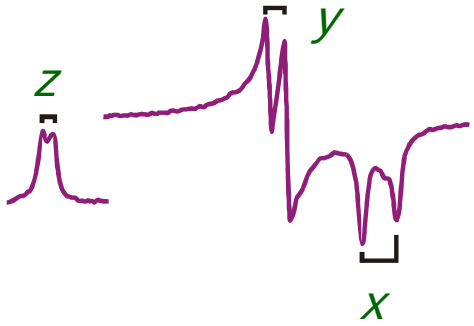

$$^{H}A = \begin{matrix} 0.39 & & \\ & 0.22 & ^{H}A_{yz} \\ & ^{H}A_{zy} & 0.13 \end{matrix} \text{ /mT}$$

C_{2v} → orthorhombic symmetry → ***g*** and ^{O}A axes coincident

C_s → monoclicic symmetry → ***g*** and ^{H}A axes noncoincident

Acknowledgement to Prof. Zbigniew Sojka
(Jagiellonian University in Krakow, Poland)

→ the local point symmetry at the given nucleus determines whether or not any of the principal axes of the g and A tensors are required to be coincident or not

accounting for the H-shf

distal dipole approximation

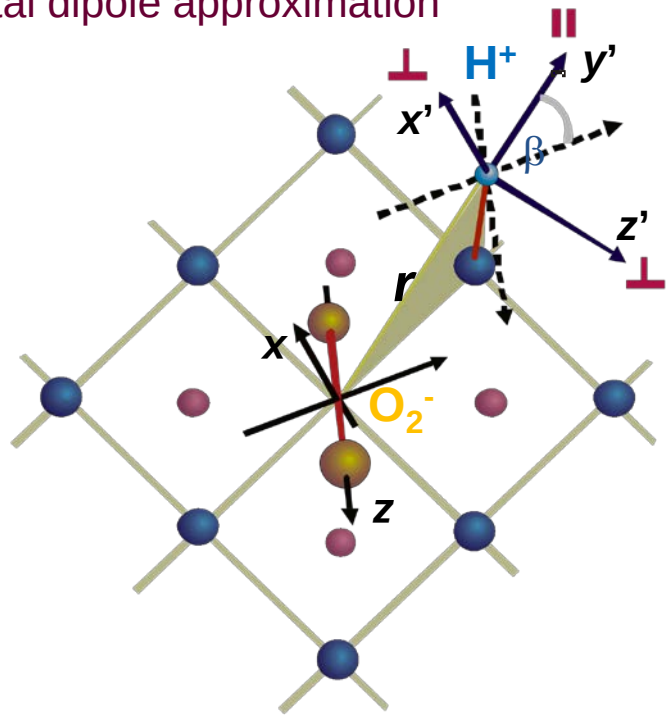

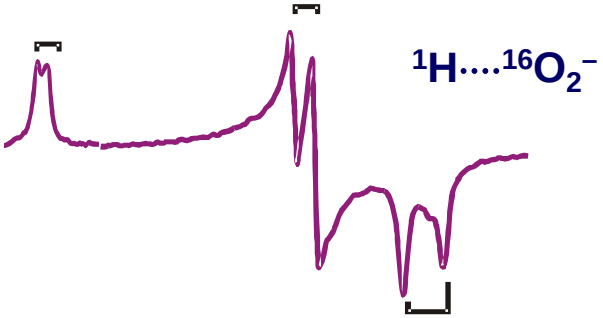

rotation formula of Hoffman (J.Mag.Res. 1984)

$$ {}^{H}A_{x'} = {}^{H}A_{x} $$

$$ {}^{H}A_{y'} = \left(\frac{{}^{H}A_{y}^{2} - ({}^{H}A_{y}^{2} + {}^{H}A_{z}^{2}) \sin^{2}\beta}{1 - 2\sin^{2}\beta} \right)^{1/2} \qquad {}^{H}A_{z'} = \left(\frac{{}^{H}A_{z}^{2} - ({}^{H}A_{y}^{2} + {}^{H}A_{z}^{2}) \sin^{2}\beta}{1 - 2\sin^{2}\beta} \right)^{1/2} $$

$$ \beta = \arcsin\left(\frac{{}^{H}A_{z}^{2} - {}^{H}A_{x}^{2}}{{}^{H}A_{y}^{2} + {}^{H}A_{z}^{2} - 2\,{}^{H}A_{x}^{2}} \right)^{1/2} $$

$A_D = {}^{H}A_{||} - a_{iso} = g_e \mu_B g_H \mu_H (3\cos^2\phi - 1)/r^3$

$r = 0.36$ nm

$r_{calc.} = 0.38$ nm

$\beta = 39^o$, ${}^{H}A_{||} = 3.2$ MHz, ${}^{H}A_{\perp} = -1.98$ MHz

Acknowledgement to Prof. Zbigniew Sojka
(Jagiellonian University in Krakow, Poland)

8th BRNO EFEPR SCHOOL

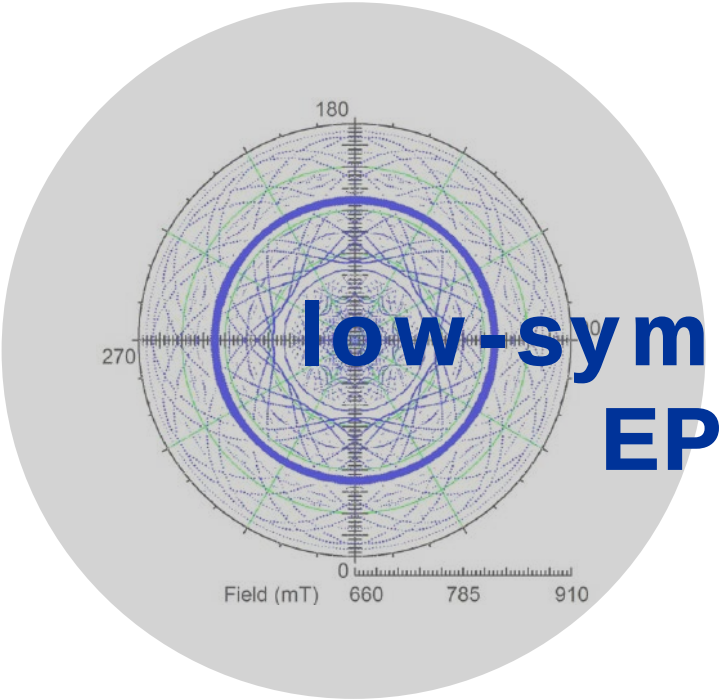

low-symmetry effects in EPR spectra

8th BRNO EFEPR SCHOOL

low symmetry complexes

low symmetry at molybdenum center

scorpionate complexes – models for molybdenum enzymes

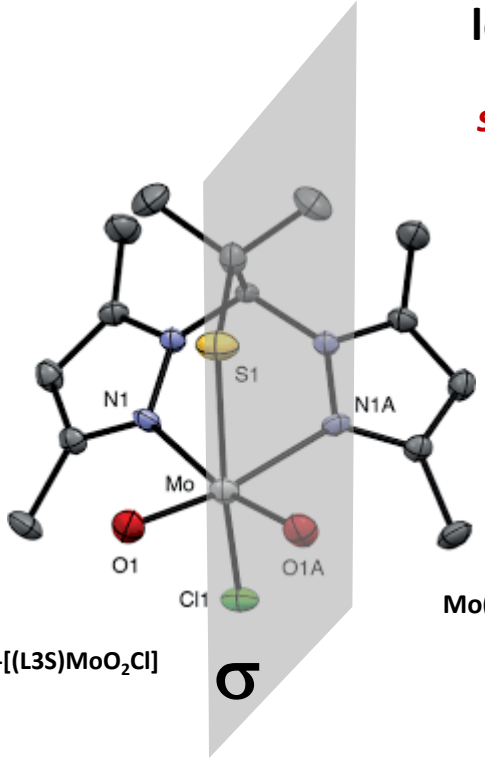

cis-[(L3S)MoO$_2$Cl]

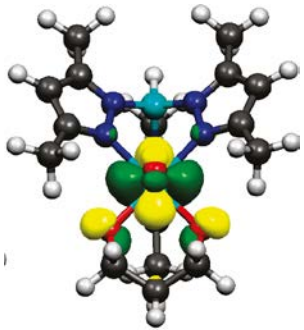

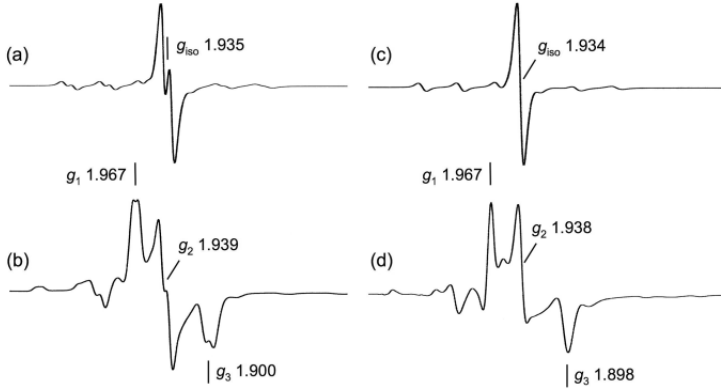

V.W.L. Ng, M.K. Taylor, J.M. White, Ch.G. Young
Inorg. Chem. 2010, *49*, 9460–9469

Mo(V) (^{95,97}Mo I = 5/2), 4d^1, S = ½, C$_s$ point symmetry (or local symmetry)

C_s	E	σ		
A’	+1	+1	x, y, R_z	x^2, y^2, z^2, xy
A’’	+1	-1	z, R_x, R_y	xz, yz

Structure after Ch. G. Young, Eur. J. Inorg. Chem. 2016, 2357-2376

measuring low symmetry

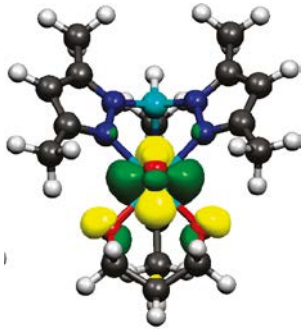

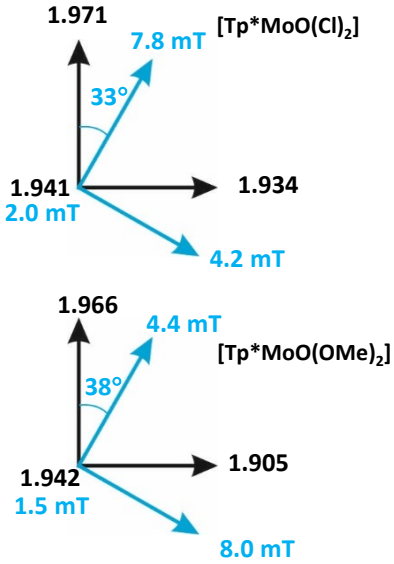

view perpendicular to mirror plane

Tris(3,5-dimethylpyrazolyl)hydroborate Mo(V) = [Tp*MoOX$_2$]

[Tp*MoO(OMe)$_2$]

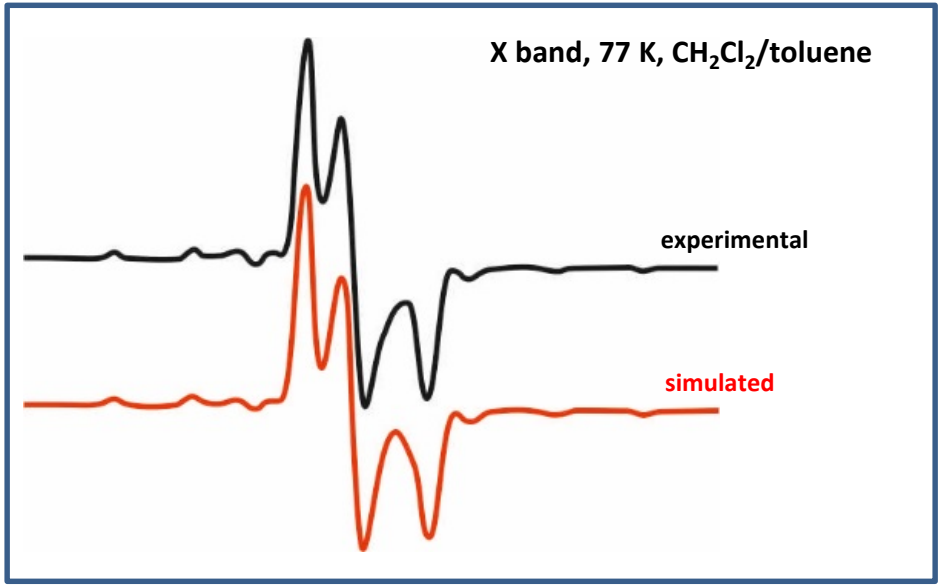

monoclinic angle defined to ± 1°

Spectra from: W.E. Cleland, K.M. Barnhart, K. Yamanouchi, D. Collison, F.E. Mabbs, R.B. Ortega, J.H. Enemark, Inorg. Chem. 1987, 26, 7, 1017-1025

non-coincidence of *g*- and *A*-tensor principal axes

$$B_{res} = \frac{h\nu_0}{g\mu_B} - \frac{Km}{g\mu_B}$$

$S = 1/2$ **$I \neq 0$**

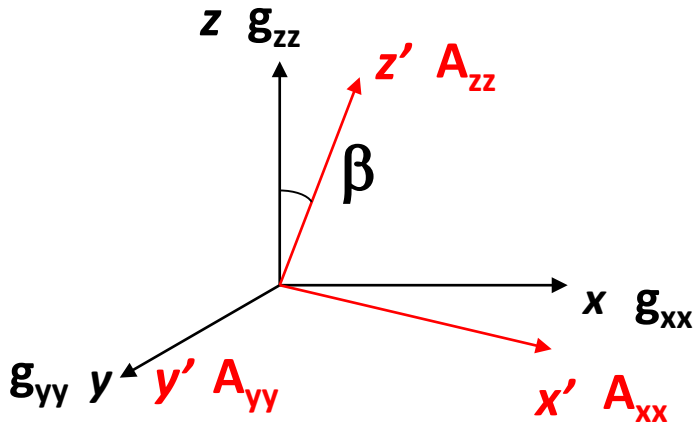

$$g = \left[\left(g_{xx}^2 \cos^2\varphi + g_{yy}^2 \sin^2\varphi\right)\sin^2\vartheta + g_{zz}^2 \cos^2\vartheta\right]^{1/2}$$

$$gK = \left[\left(g_{xx}^2 A_{xx}^2 \cos^2\phi + g_{yy}^2 A_{yy}^2 \sin^2\phi\right)\sin^2\vartheta + g_{zz}^2 A_{zz}^2 \cos^2\vartheta\right]^{\frac{1}{2}}$$

$$K \approx \left[A_x^2 \sin^2(\theta-\beta) + A_z^2 \cos^2(\theta-\beta)\right]^{\frac{1}{2}}$$

consider transition in the xz plane

non-coincidence of *g*- and *A*-tensor principal axes

$$K \approx \left[A_{xx}^2 \sin^2(\vartheta-\beta) + A_{zz}^2 \cos^2(\vartheta-\beta)\right]^{\frac{1}{2}}$$

$$\frac{\partial B(\vartheta,\varphi)}{\partial \vartheta} = 0 \qquad \textit{for } \theta \textit{ given by}$$

$$\tan 2\vartheta = \frac{\sin 2\beta}{F + \cos 2\beta} \qquad F = \left(\frac{g\mu_B B}{mK}\right)\left(\frac{g_{xx}^2 - g_{zz}^2}{A_{xx}^2 - A_{zz}^2}\right)\left(\frac{K^2}{g^2}\right)$$

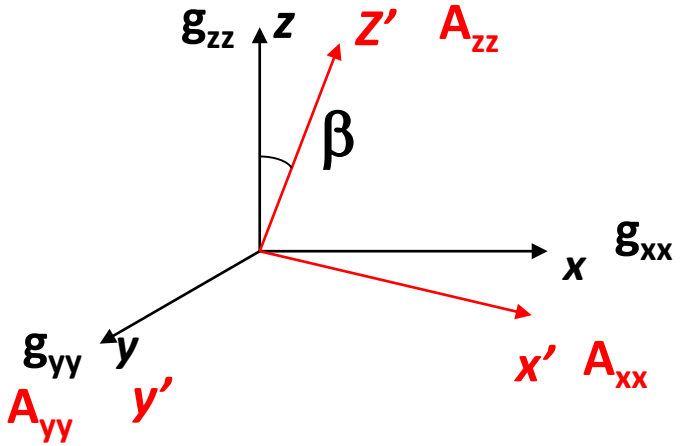

when $\beta = 0$ *or* $\Delta g >> \Delta A$ $\Rightarrow F >> 1 \Rightarrow tan\,2\vartheta = 0 \Rightarrow$ spectral features at θ = 0° and 90° (along *g* principal axes)

when $\Delta A >> \Delta g \Rightarrow tan\,2\vartheta = tan\,2\beta$ features appear along *A* principal axes (θ = 0° and β)

J. Am. Chem. Soc. 102, 156, 1980; 106, 7000, 1984.

for F = 1 the resonant field becomes a function of g_{xx}, g_{zz}, A_{xx}, A_{zz}, and β

the non-coincidence effects on an EPR powder spectrum become obvious if two (or more) tensors have relevant and comparable anisotropies between them

non-coincidence of *g*- and *A*-tensor principal axes

Effects of non-coincidence of tensors *g* and *A* on a powder spectrum:

1) the spectrum contains „too many lines”
2) the intensity and position of the spectral lines is not that expected on the basis of simple considerations
3) it is not possible to simulate the spectrum assuming rhombic or axial symmetry

non-coincidence of *g*- and *A*-tensor principal axes

g_{xx} = 2.000 $|A_{xx}|$ = 15 mT

g_{yy} = 1.950 $|A_{yy}|$ = 2.5 mT

g_{zz} = 1.900 $|A_{zz}|$ = 2.5 mT

I = 7/2

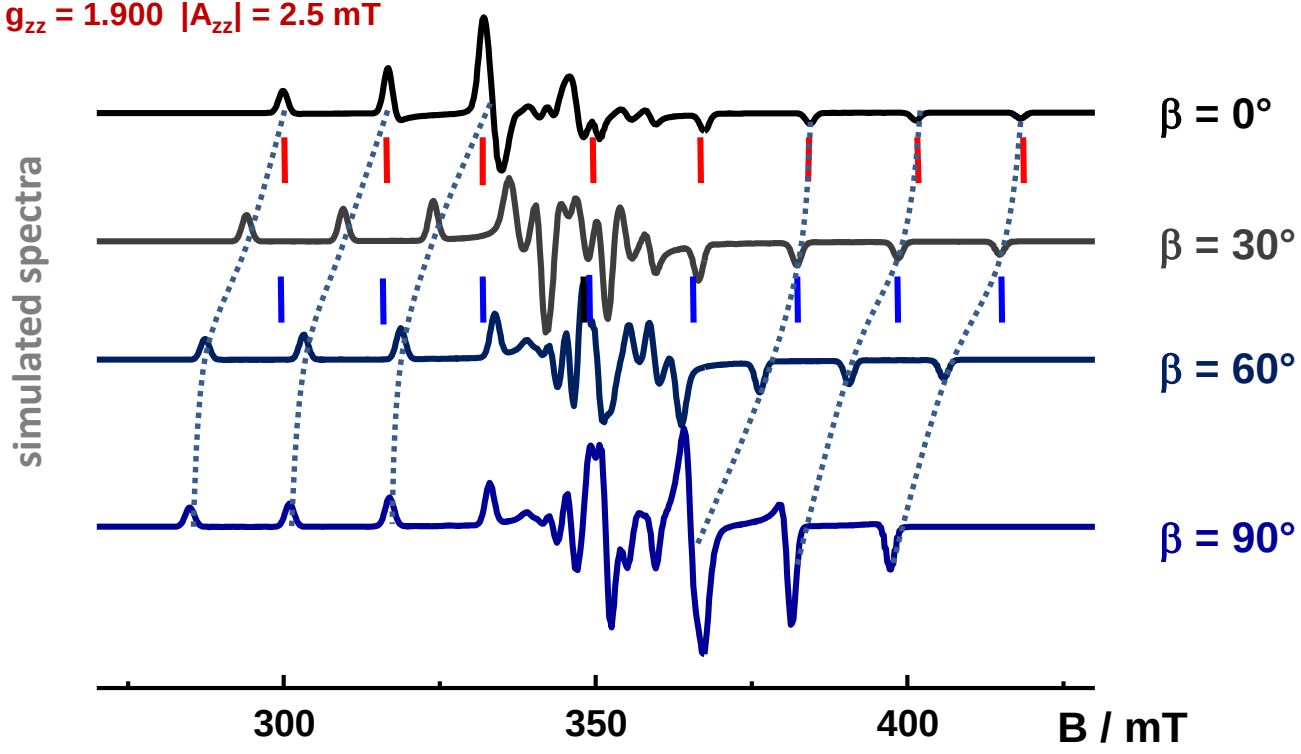

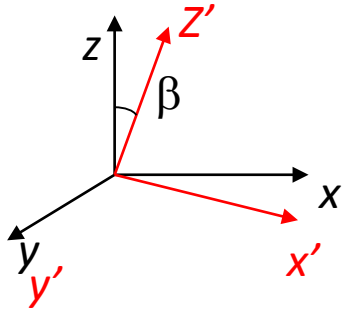

low-symmetry features

low symmetry

non-coincidence of *g*- and *A*- axes

irregular hyperfine separation

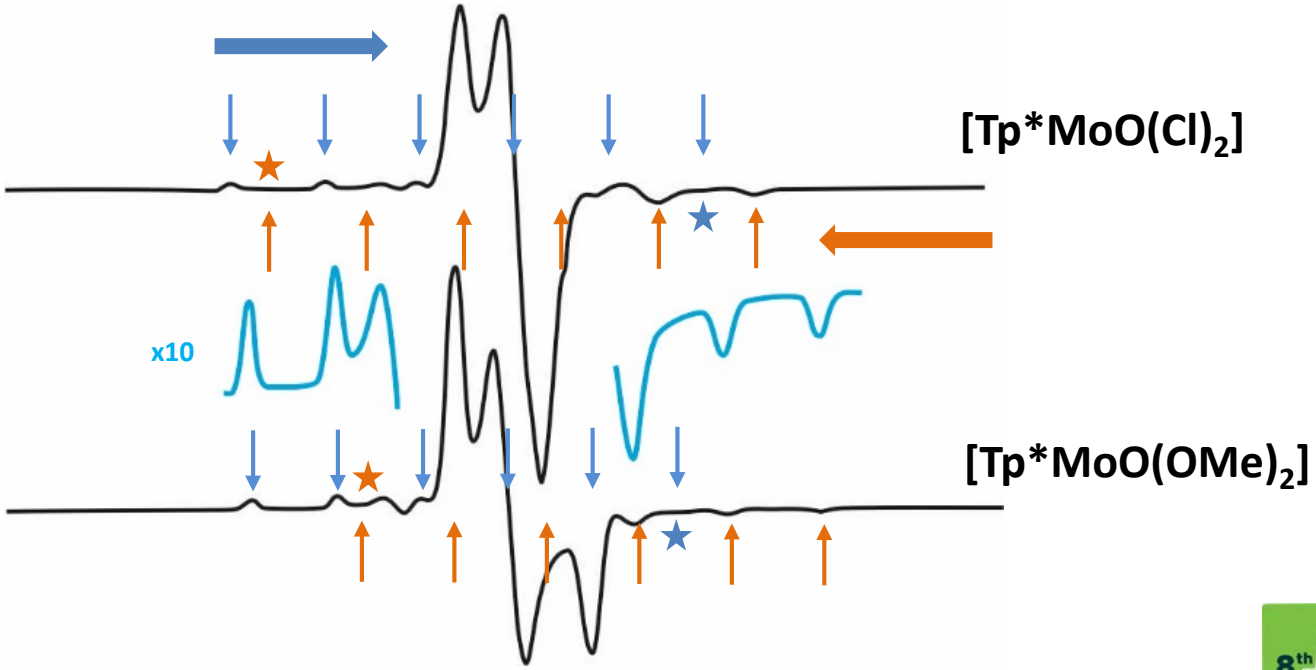

Spectra from: W.E. Cleland, K.M. Barnhart, K. Yamanouchi, D. Collison, F.E. Mabbs, R.B. Ortega, J.H. Enemark, Inorg. Chem. 1987, 26, 7, 1017-1025

8th BRNO EFEPR SCHOOL

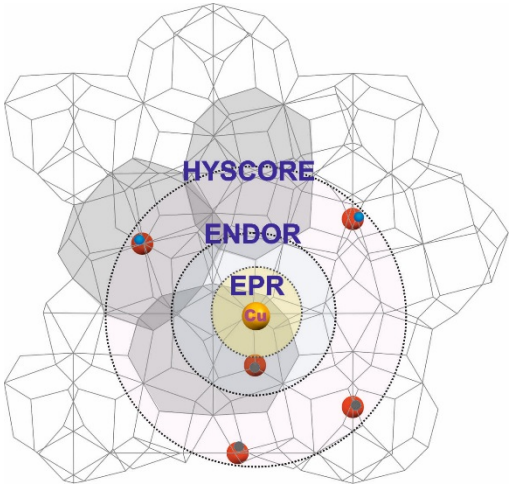

Local inhomogeneity and local symmetry probes

strain broadening and smearing of EPR features

Cu-ZSM-5 zeolite

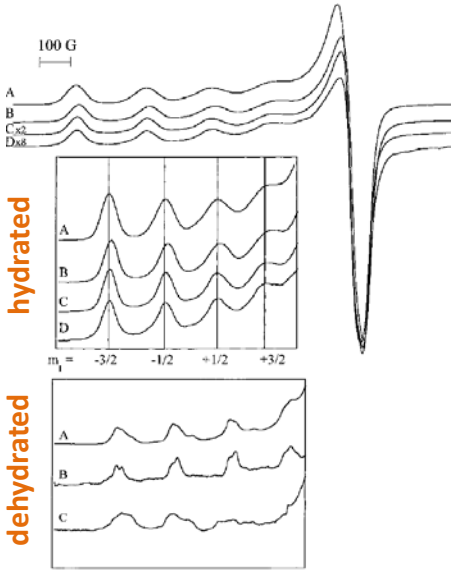

Spectra from: P.J. Carl, S.C. Larsen, J. Phys. Chem. B 2000, *104,* 6568-6575

g-strain

Powder samples come with a distribution of local surroundings (conformations) of the paramagnetic centers

For EPR this means that a paramagnetic center, which has a slightly different structural surrounding, exhibits a slightly different *g*-value.

This structural inhomogeneity is a source of the so called *g-strain*, and is reflected in the spectroscopy in the form of an inhomogeneous line shape.

This normally results in a change from a *Lorentzian* to *Gaussian* line shape. An important consequence of this *g*-strain effect is that the line width is in general, also anisotropic.

hydrated MnK-A zeolite (0.1 wt.% Mn)

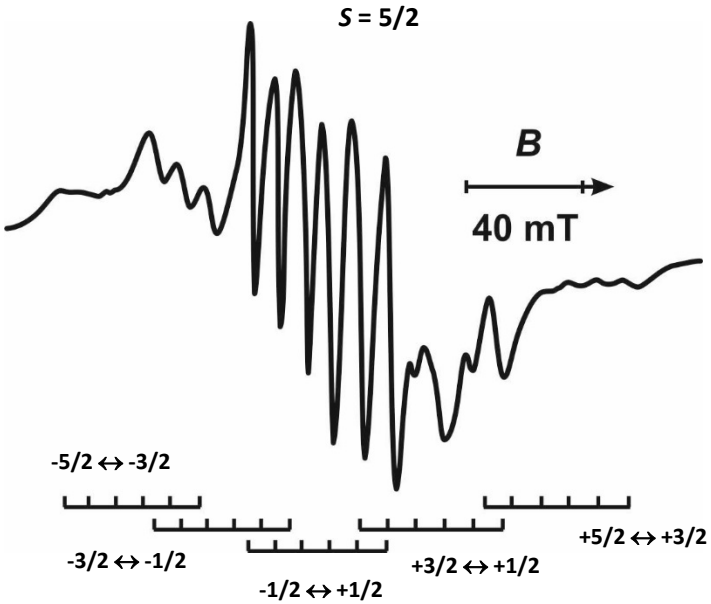

Spectrum from: D.E. De Vos, B.M. Weckhuysen, T. Bein, J. Am. Chem. Soc., 1996, 118, 9615–9622.

8th BRNO EFEPR SCHOOL

strain broadening and smearing of EPR features

g-strain

In magnetically diluted systems *g*-strain (but also *A*- and *D*-strains) leads to apparent m_I and frequency dependence of the hyperfine (and fine) linewidths (σ):

$$\sigma_\nu^2 = \left(\sum_{i=x,y,z} \left\{ \sigma_{R_i}^2 \left[\frac{\Delta g_i}{g_i} \nu_0(B) + \Delta A_i m_I \right]^2 \right\} g_i^2 l_i^2 \right) / g^2$$

σ_{Ri} are the residual linewidths due to unresolved metal and (or) ligand hyperfine splitting, homogeneous broadening and other sources;
Δg_i and ΔA_i are the widths of the Gaussian distributions of the *g* and *A* values

J. Magn. Reson. 1991, 93, 12

hydrated MnK-A zeolite (0.1 wt.% Mn)

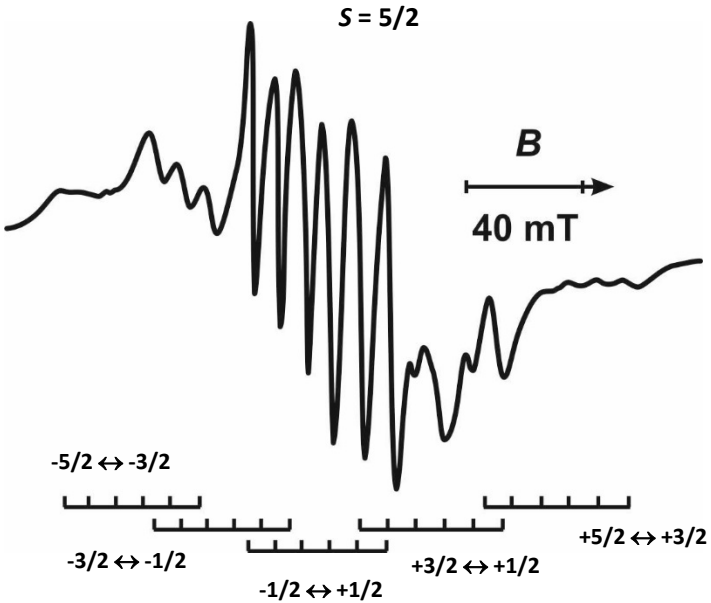

Spectrum from: D.E. De Vos, B.M. Weckhuysen, T. Bein, J. Am. Chem. Soc., 1996, 118, 9615–9622.

strain broadening and smearing of EPR features

MoO_x/SiO_2 catalysts

Spectra from: M. Che, J.C. McAteer, A.J. Tench
J. Chem. Soc., Faraday Trans. 1, 1978,**74**, 2378-2384

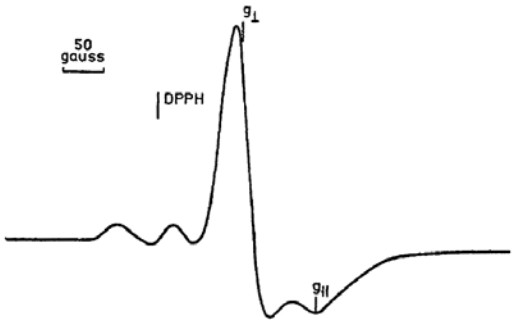

X-band, 25°C, reduction in H_2 at 500°C

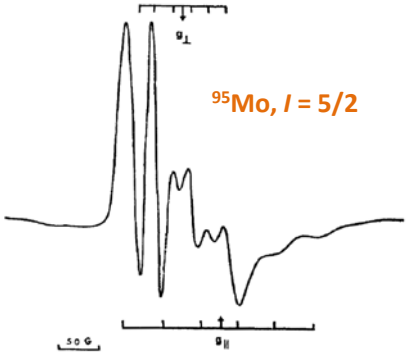

^{95}Mo, $I = 5/2$

^{95}Mo-enrichment
X-band, 25°C, reduction in H_2 at 500°C

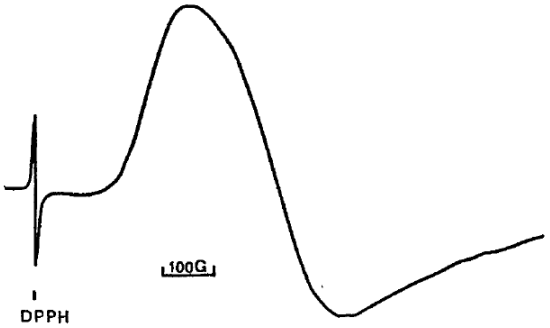

^{95}Mo-enrichment
Q-band, 25°C, reduction in H_2 at 500°C

g-strain refers to anisotropic broadening of the linewidths owing to distribution of g-values caused by small local inhomogeneity (slight variations in the orientation of the Mo(V) surface centers, heteroleptic various surface ligands, geometric strains, surface strains). Also, broadening of the g-values depends on the microwave frequency. If the line broadening were determined only by *e.g.* unresolved hyperfine coupling (which are field-independent), then the line widths would also be field independent, but they often are not.

use of local paramagnetic probes

Mayenite

$12CaO \cdot 7Al_2O_3$
unit cell = 12 cages
charge of unit cell = +4

SEM image

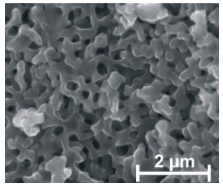

mayenite cage with O_2^- counterion

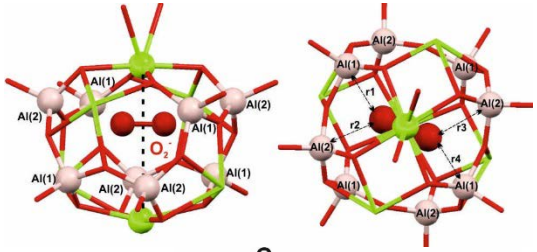

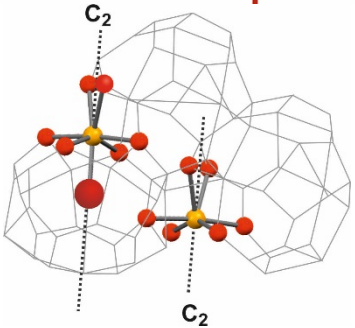

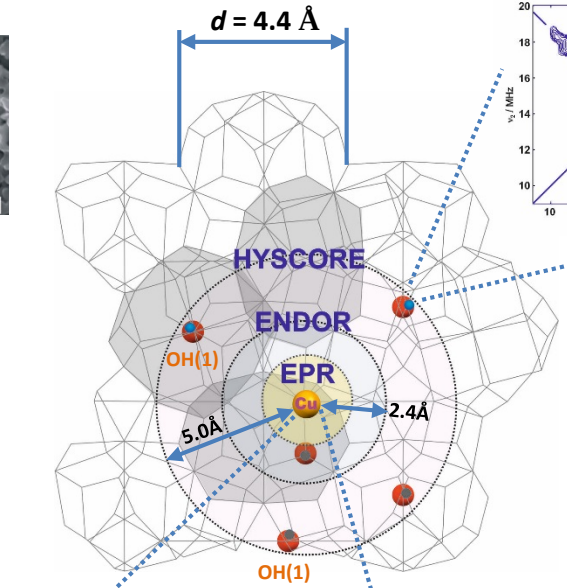

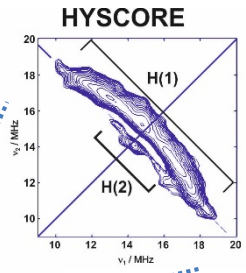

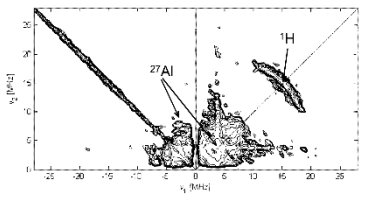

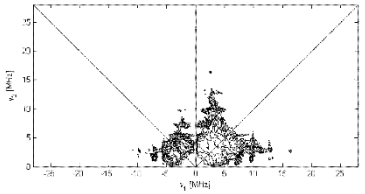

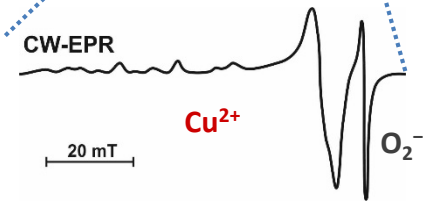

$$T = (\mu_0/4\pi) g_e g_n \mu_B \mu_n (1/r^3)$$

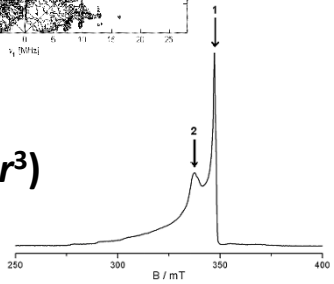

S. Maurelli, M. Ruszak, S. Witkowski, P. Pietrzyk, M. Chiesa, Z. Sojka
Phys. Chem. Chem. Phys. 2010, 12, 10933-10941

8th BRNO EFEPR SCHOOL

local symmetry probe (*g* tensor)

$$g_{ij} = g_e \delta_{ij} - 2\lambda \Lambda_{ij} \qquad \Lambda_{ij} = \Lambda_{ji} = \hbar^{-2} \sum_{n \neq 0} \frac{\langle 0|L_i|n\rangle\langle n|L_j|0\rangle}{E_n - E_0}$$

λ – *stała sprzężenia spinowo-orbitalnego*

$\Gamma_0 \times \Gamma_L \times \Gamma_n \subset$ **totally symmetric representation** Γ_A

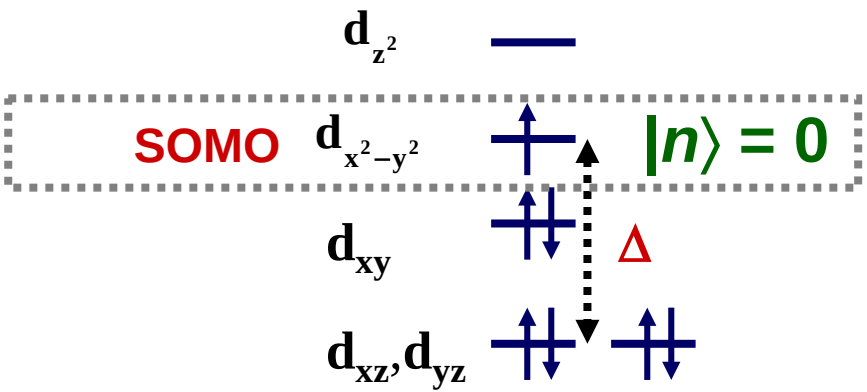

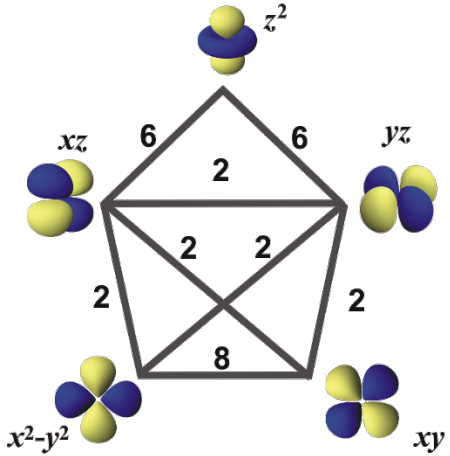

$$g = 2.0023 \pm n\lambda/\Delta$$

local symmetry probe

isotropic center

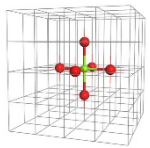

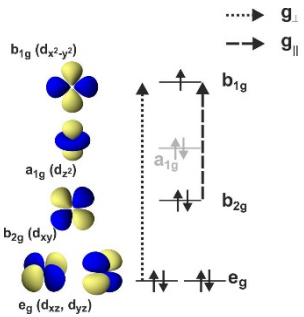

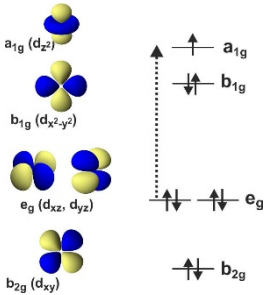

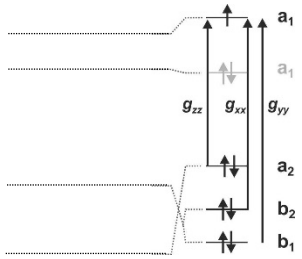

axial distortion

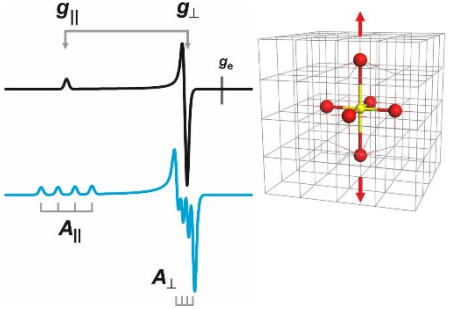

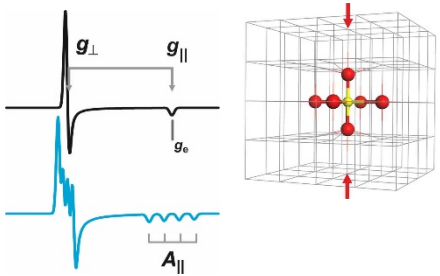

$$g_\parallel = g_e + \frac{8\lambda}{E_{x^2-y^2} - E_{xy}} \qquad g_\perp = g_e + \frac{2\lambda}{E_{x^2-y^2} - E_{xz,yz}}$$

$$g_\perp = g_e + \frac{6\lambda}{E_{z^2} - E_{xz,yz}}$$

$$g_\parallel \approx g_e$$

rhombic distortion

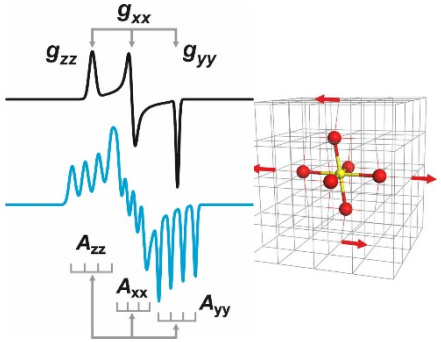

local symmetry probe

differentiation between d^1 and d^9 configurations

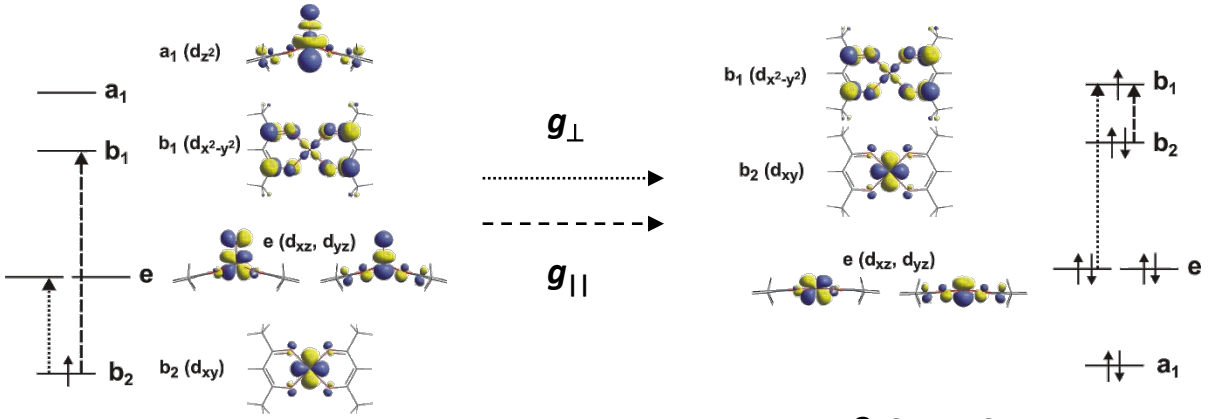

$3d^1$ (Ti^{3+})

coupling with empty (virtual) d states (negative g-shift)

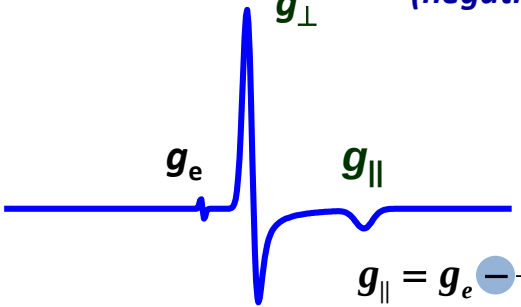

$$g_{\parallel} = g_e - \frac{8\lambda}{E_{x^2-y^2} - E_{xy}}$$

$3d^9$ (Ni^{+})

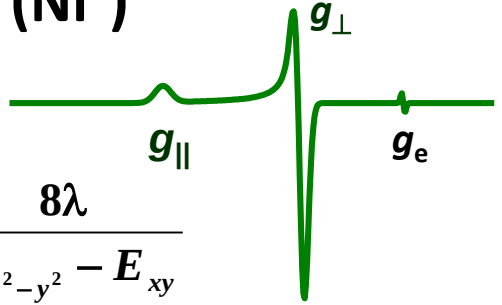

$$g_{\parallel} = g_e + \frac{8\lambda}{E_{x^2-y^2} - E_{xy}}$$

coupling with occupied d states (positive g-shift)

local symmetry probe

Axial symmetry
2 nearly equivalent Cu(II) centers
Antiferromagnetic coupling

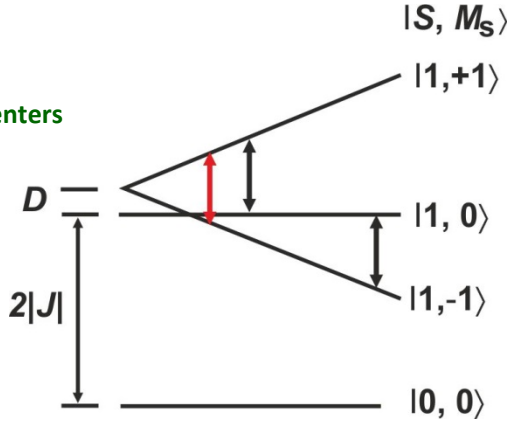

$\Delta M_S = \pm 2$

CeO_2 matrix

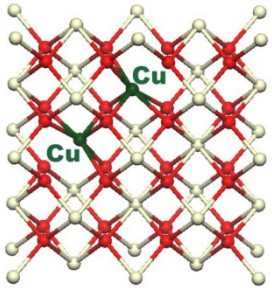

Cu(II)-$(O^{2-})_2$-Cu(II)

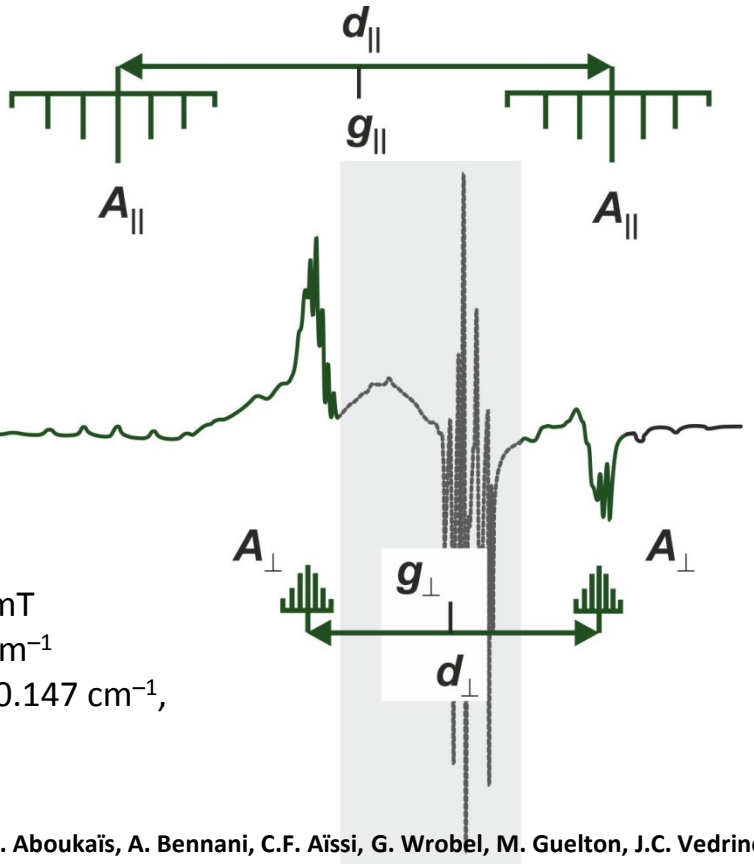

$g_{\parallel} = 2.2079$, $g_{\perp} = 2.0403$
$|A_{\parallel}| = 8.5$ mT, $|A_{\perp}| = 1.35$ mT
$D = 0.066$ cm^{-1}, $J = -52.5$ cm^{-1}
$d_{\text{Cu-Cu}} = -0.081$ cm^{-1}, $D^{(S)} = 0.147$ cm^{-1},

$$\boldsymbol{H}_{EX} = \hbar^{-2} \sum_{AB} \left[-J \boldsymbol{S}_A \boldsymbol{S}_B + \boldsymbol{d}_{AB} \left(\boldsymbol{S}_A \times \boldsymbol{S}_B \right) + \boldsymbol{S}_A \boldsymbol{D}^{(S)}{}_{AB} \boldsymbol{S}_B \right]$$

Isotropic exchange term | Antisymmetric ex. term (D.-M.) | Symmetric ex. term

Spectrum from A. Aboukaïs, A. Bennani, C.F. Aïssi, G. Wrobel, M. Guelton, J.C. Vedrine, *J. Chem. Soc., Faraday Trans. I*, 1992, 88, 615

Conclusions

Analysis of EPR spectra of powder samples requires:

1. computer simulations
2. accounting for EPR parameters strains
3. accounting for low-symmetry effects
4. checking for presence of off-axis extra features

Useful experiments and procedures

adsorption of probe molecules
isotopic substitution
multifrequency measurements
use of hyperfine techniques

References and further reading

1. John A. Weil, James R. Bolton, *Electron Paramagnetic Resonance: Elementary Theory and Practical Applications*, 2007 John Wiley & Sons, Inc.
2. F. Mabbs, D. Collison, *Electron Paramagnetic Resonance of d Transition Metal Compounds*, Elsevier Amsterdam, 1992
3. M. Brustolon, E. Giamello, (Ed), *Electron Paramagnetic Resonance. A Practitioner's toolkit.* 2009, John Wiley & Sons, Hoboken, 2009.
4. J. R. Pilbrow, *Transition Ion Electron Paramagnetic Resonance*, Oxford University Press, Oxford, 1990.

5. P. Pietrzyk, Z. Sojka, E. Giamello, *in Characterization of Solid Materials and Heterogeneous Catalysis – From Structure to Surface Reactivity*, M. Che, J. C. Védrine (Ed), Wiley-VCH, Weinheim, 2012, p. 343.
6. P. Pietrzyk, T. Mazur, Z. Sojka, Local Structural Characterisation: Inorganic Materials Series, John Wiley & Sons, 2014, p. 225.
7. Ph. Rieger, *Electron Spin Resonance. Analysis and Interpretation.*, RSC Publishing, Cambridge, 2007.
8. R. S. Drago, *Physical methods for chemists*, Saunders College Pub., 1992

9. I.V. Ovchinnikov, V. N. Konstantinov, *J. Magn. Reson.*, 1979, 32, 179.
10. B. M. Peake, Ph. H. Rieger, B. H. Robinson, J. Simpson, *J. Am. Chem. Soc.*1980, 102, 156-163; W. E. Geiger, Ph. H. Rieger, B. Tulyathan, M. D. Rausch, *J. Am. Chem. Soc.*1984, 106, 7000-7006.
11. A. Kreiter, J. Hatermann, *J. Magn. Reson.* 1991, 93, 12-26

Thanks for your attention!

8th BRNO EFEPR SCHOOL

CEITEC

www.eprschool.ceitec.cz

EFEPR